Western Michigan University
ScholarWorks at WMU

Masters Theses

Graduate College

8-1968

A Study of the 16.7 MeV Level of the ^{5}He

James David George
Western Michigan University

Follow this and additional works at: https://scholarworks.wmich.edu/masters_theses

Part of the Nuclear Commons

Recommended Citation

George, James David, "A Study of the 16.7 MeV Level of the ^{5}He" (1968). *Masters Theses*. 3152.
https://scholarworks.wmich.edu/masters_theses/3152

This Masters Thesis-Open Access is brought to you for free and open access by the Graduate College at ScholarWorks at WMU. It has been accepted for inclusion in Masters Theses by an authorized administrator of ScholarWorks at WMU. For more information, please contact wmu-scholarworks@wmich.edu.

A STUDY OF THE 16.7 MeV LEVEL OF ^5He

by

James David George

A Thesis
Submitted to the
Faculty of the School of Graduate
Studies in partial fulfillment
of the
Degree of Master of Arts

Western Michigan University
Kalamazoo, Michigan
August 1968

Reproduced with permission of the copyright owner. Further reproduction prohibited without permission.

ACKNOWLEDGEMENTS

Gratitude and appreciation is expressed to Professor R. E. Shamu for his guidance and assistance, without which this project could not have been accomplished. Thanks are also due to Mr. J. Meagher and Mr. K. Williams of the Western Michigan University Computer Center for their assistance with the calculations.

Discussions with Professors G. Hardie, L. D. Oppliger, and G. E. Bradley were very helpful. The interest and encouragement shown by the rest of the faculty of the Department of Physics has been greatly appreciated. It has been an enjoyable privilege and experience working with these men for the past two years.

Special thanks is also due to my wife, Sharon, for her patience and assistance in preparing the manuscript.

James David George

Reproduced with permission of the copyright owner. Further reproduction prohibited without permission.

MASTER'S THESIS M-1652

GEORGE, James David
A STUDY OF THE 16.7 MeV LEVEL OF ^{5}He.

Western Michigan University, M.A., 1968
Physics, nuclear

University Microfilms, Inc., Ann Arbor, Michigan

Reproduced with permission of the copyright owner. Further reproduction prohibited without permission.

TABLE OF CONTENTS

Reproduced with permission of the copyright owner. Further reproduction prohibited without permission.

Reproduced with permission of the copyright owner. Further reproduction prohibited without permission.

FIGURES AND TABLES

FIGURES | Page

Reproduced with permission of the copyright owner. Further reproduction prohibited without permission.

Reproduced with permission of the copyright owner. Further reproduction prohibited without permission.

INTRODUCTION

One of the fundamental problems of nuclear physics is the study of charge symmetry, that is, the comparison of the neutron-neutron interaction and the nuclear part of the proton-proton interaction. One can define two versions of charge symmetry which shall be called the weak statement and the strong statement[1]. The weak statement, pertaining to the interaction between only two nucleons, is the hypothesis that the neutron-neutron interaction is the same as the nuclear part of the proton-proton interaction. The weak statement is the one tested by comparing parameters obtained from proton-proton scattering with parameters obtained from studies of the neutron-neutron interaction. The strong statement implies the first and pertains to the interaction between two nucleons in nuclei containing more than two nucleons. It asserts that one may simultaneously exchange all neutrons for protons and all protons for neutrons in any experiment and obtain the same result[1]. There is strong evidence available to indicate that the weak statement is indeed valid[2,3]. Although there is also evidence which supports the strong statement of charge symmetry, there is some question concerning the degree of its correctness.

There are several arguments which support the strong statement of charge symmetry. The fact that the number of neutrons plus the number of protons is approximately equal in the nuclei of the elements is evidence for the correctness of this assumption[4]. If either the neutron-neutron or proton-proton force were much greater

Reproduced with permission of the copyright owner. Further reproduction prohibited without permission.

than the other, then nuclei would exist of purely protons or purely neutrons. One must note, however, that as the atomic number increases, the ratio of neutrons to protons also increases. It is felt that this neutron excess may be adequately explained by considering the short range of the nuclear force and the long range of the Coulomb repulsion between pairs of protons[4].

The properties of mirror nuclei are also evidence for the strong statement of charge symmetry[1]. Two nuclei are called mirror nuclei if one has the same number of neutrons as the other has protons and the same number of protons as the other has neutrons. See Figures I and II for examples of mirror nuclei level structure. However, it is still unclear if the shift in energy level structure of mirror nuclei is due entirely to the additional Coulomb energy in the nuclei with the greater number of protons[1]. And, it is not clear that the increase in the ratio of neutrons to protons in the heavier nuclei is due entirely to the Coulomb repulsion[4]. Thus it is possible that part of the shift in the energy level structure and that part of the increased ratio of neutrons to protons in the heavier nuclei may be caused by a difference between the neutron-neutron force and the proton-proton force in the nucleus.

Because of the fundamental nature of charge symmetry, it is of interest to determine if a small difference does exist between the neutron-neutron and the proton-proton forces in nuclei. And if so, it would be important to determine the magnitude and the effects of the difference in the interaction.

Reproduced with permission of the copyright owner. Further reproduction prohibited without permission.

Figures I and II. Energy Level Structure of ^5He and ^5Li. Energy values are plotted vertically in MeV, based on the ground state as zero. Uncertain levels are indicated by dashed lines; levels which are known to be particularly broad are cross hatched. The levels and parity are indicated in the standard spectroscopic notation. For reactions in which ^5He or ^5Li is the compound nucleus, some typical thin-target excitation functions are shown schematically, with the yield plotted horizontally and the bombarding energy vertically. Bombarding energies are included in laboratory coordinates and plotted to scale in center-of-mass coordinates.

Reproduced with permission of the copyright owner. Further reproduction prohibited without permission.

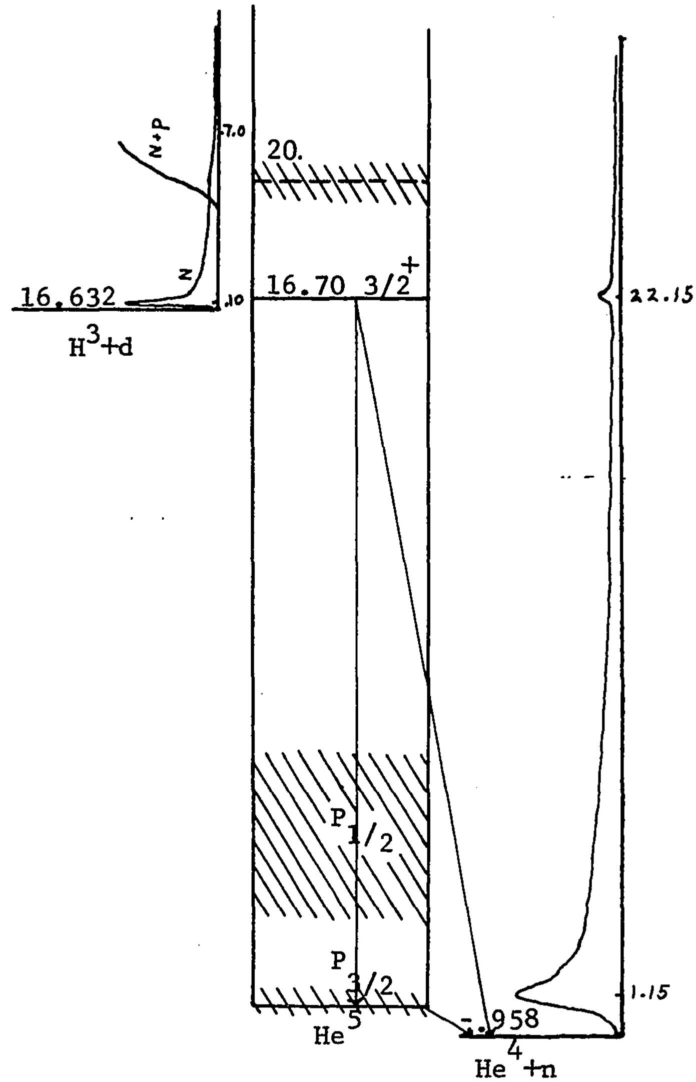

Figure I

Reproduced with permission of the copyright owner. Further reproduction prohibited without permission.

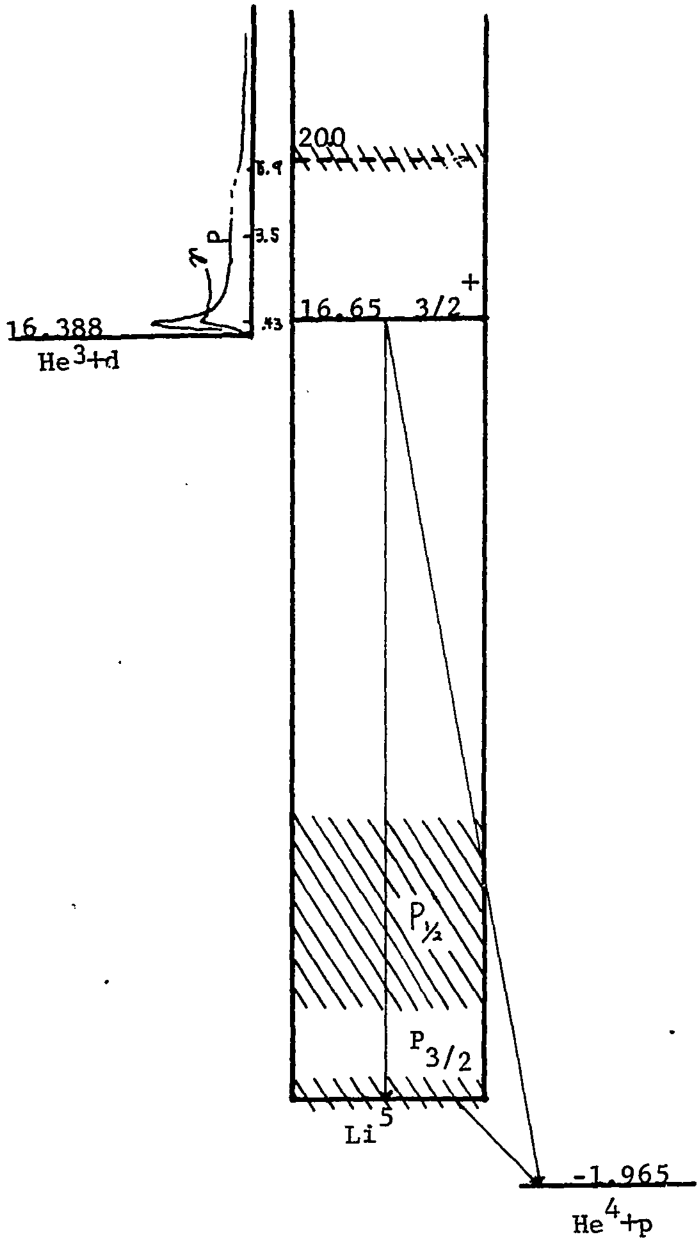

Figure II

Reproduced with permission of the copyright owner. Further reproduction prohibited without permission.

One procedure that has been attempted by several investigators[5,6,7] is an examination of the nuclear parameters--the reduced widths and resonance energies--of a sharp resonant level in mirror nuclei. The strong statement of charge symmetry predicts the nuclear parameters for two analogue levels in mirror nuclei to be the same.

A convenient mirror pair for study is ^5He and ^5Li as they are relatively simple. Both systems exhibit similiar level structures and both have an isolated sharp resonance at approximately 17 MeV above the ground state[8]. The relatively isolated sharp resonance allows the use of the rather straightforward single level resonance theory. One disadvantage that this pair of mirror nuclei has is that the thresholds of the deuteron+triton reaction in ^5He and the deuteron + ^3He reaction in ^5Li, occur just below the resonance, which complicates the analysis somewhat.

A number of previous investigators[6,9,10,11] have determined values for the reduced widths for the two systems. Table I presents the results of some of these investigations. In this table γ_n^2 is the reduced width of the neutron, γ_p^2 is the reduced width of the proton, and γ_d^2 is the reduced width of the deuteron.

Of the three parameters listed, the parameter g will be examined in the following analysis because it can be determined with less uncertainty[11] than the values of γ_n^2, γ_p^2 or γ_d^2. If the strong statement of charge symmetry is valid, g will be the same for both ^5He and ^5Li. It is seen from Table I that at present there is

Reproduced with permission of the copyright owner. Further reproduction prohibited without permission.

Table I

Level Parameters for the $3/2^+$ Level in

^5He (16.67 MeV) and ^5Li (16.7 MeV)

Interaction radius: $r = 5.0 \times 10^{-13}$ cm

He^5 System

γ_n^2 (MeV)	γ_d^2 (MeV)	$g = \gamma_d^2 / \gamma_n^2$	Experimental Data
.0555	2.00	36[6]	Total T (d,n) He^4 Reaction Cross Section[6]
.0500	2.00	40[10]	Total Scattering Cross Section[17]
			Total d (T,n) He^4 Reaction Cross Section[12]
.0742	3.34	45[9]	Total T (d,n) He^4 Reaction Cross Section[6]
			Total d + T Elastic Scattering at 90°[27]

Reproduced with permission of the copyright owner. Further reproduction prohibited without permission.

Table I Cont.

^{5}Li System

γ_p^2 (MeV)	γ_d^2 (MeV)	$g = \gamma_d^2/\gamma_n^2$	Experimental Data
.0742	3.34	45[9]	d + He^3 Elastic Scattering at 90°[9]
			Ave. Total He^3 (d,p) He^4 Cross Section[13,14]
.0264	1.4	53[11]	Total He^3(d,p)He^4 Cross Section[13]
.0334	1.50	45[11]	Ave. Total He^3 (d,p) He^4 Cross Section[13,18]
			p - α Differential Cross Section vs Energy[15,25]
			Polarization[11,16,26]
.0428	3.0	70[11]	Ave. Total He^3 (d,p) He^4 Cross Section[7,17,19]
			p - α Differential Cross Section vs Energy[25,15]
			Polarization[11,16]

Reproduced with permission of the copyright owner. Further reproduction prohibited without permission.

large disagreement in the value of g both for ^5He and ^5Li. It may be that some of the comparisons examined were not overly sensitive to the nuclear parameters[+]. The situation for ^5Li is further complicated because existing measurements[7,13,14,17,18,19] of the He^3 (d,p) He^4 reaction cross section do not agree[11]. It is seen that the analyses listed in Table I indicate that the strong form of charge symmetry may be valid, e. g. if g = 45 for both ^5Li and ^5He. However, because of the uncertainty in the value of g for both ^5He and ^5Li, to date, this validity has not been proven.

This work is a re-examination of the nuclear parameters for the sharp resonance in ^5He at 16.7 MeV above ground state. In neutron-alpha scattering the level in ^5He is observed as an anomaly in the scattering cross section[20,21]. Neutron-alpha differential cross section data which have not previously been used for comparison to determine the nuclear parameters are available[20]. Comparisons of these data to single level resonance theory calculations are made for various values of g. Comparisons are made for the total scattering cross section[++], the differential elastic scattering cross section, and the polarization for neutron-alpha scattering. Particular emphasis is placed on the differential

---

[+]It has been suggested by Breit[5] that an analysis based only on total reaction cross sections may not be overly sensitive in determining the reduced widths.

[++]The total scattering cross section is defined as the sum of the total elastic scattering cross section, He^4 (n,n) He^4, and the total reaction cross section, He^4 (n,d) T.

Reproduced with permission of the copyright owner. Further reproduction prohibited without permission.

elastic scattering cross section. The polarization[22] and the angle of rotation of spin[+] will be examined to see if either measurement is a sensitive test for the nuclear parameters.

It is the purpose of this thesis to determine the nuclear parameters for the 16.7 MeV level in ^{5}He using existing data[20]. These parameters will be compared with the suggested values for the analogue state in ^{5}Li.

An analysis of the polarization and rotation parameter will also be performed to see if these measurements are suitable to further substantiate the values of g for the resonant level in ^{5}He.

[+]The angle of rotation of spin may be determined by means of a triple scattering experiment where the plane of the second scattering is perpendicular to the plane of the first scattering[23,24].

Reproduced with permission of the copyright owner. Further reproduction prohibited without permission.

THEORY

The scattering of nucleons by a nucleus may be described by the method of partial waves. If, for the moment, one neglects spin, then the incident beam of neutrons may be represented, to a good approximation, by a plane wave of the form e^{ikz} where k represents the magnitude of the propagation vector in the center-of-mass system and z is measured along the direction of propagation[28]. This plane wave may also be expressed as a sum of partial waves:

$$e^{ikz} = e^{ikr\cos\theta} = \sum_{\ell=0}^{\infty} a_\ell \, J_\ell(kr) \, P_\ell(\cos\theta)$$

where $a_\ell = (2\ell + 1)\, i^\ell$, $J_\ell\ (k\,r)$ = spherical Bessel function, and $P_\ell\ (\cos\theta)$ = Legendre polynomial of order ℓ. In this representation, the plane wave of linear momentum has been decomposed into an infinite series of partial waves, each of differing angular momentum ℓ.

When analyzing scattering phenomena by the method of partial waves, it is convenient to introduce the concept of a phase shift. The term phase shift refers to a shift in phase which an incident partial wave undergoes upon scattering[28]. All of the quantities which one may measure in a scattering experiment may be expressed in terms of phase shifts. As given by Burke[29], the differential elastic scattering cross section, $\frac{d\sigma}{d\Omega}$, the polarization, $P_\ell(\theta)$, and the angle of rotation of spin, β, may be calculated from the phase shifts, for a neutron incident on an alpha particle as:

Reproduced with permission of the copyright owner. Further reproduction prohibited without permission.

$$\frac{d\sigma}{d\Omega}(\theta) = \frac{1}{k^2}\left[|A|^2 + |B|^2 \right] \qquad 1$$

$$P(\theta) = \frac{2\, Im\,(A^* B)}{|A|^2 + |B|^2} \qquad 2$$

$$\beta = \arctan\left[\frac{2\, Re\,(B^* A)}{|A|^2 + |B|^2} \right] \qquad 3$$

where A and B are respectively the coherent and incoherent scattering amplitudes,

$$A = \sum_{\ell=0}^{\ell_{max}} \left[(\ell+1) f_\ell^+ + \ell f_\ell^- \right] P_\ell(\cos\theta) \qquad 4$$

$$B = \sum_{\ell=0}^{\ell_{max}} \left[f_\ell^- - f_\ell^+ \right] \frac{d}{d(\cos\theta)} P_\ell(\cos\theta) \qquad 5$$

The partial scattering amplitudes, $f_\ell^\pm$, are related to the phase shifts, $\delta_\ell^\pm$, by

$$f_\ell^\pm = \frac{e^{2i\delta_\ell^\pm} - 1}{2i} \qquad 6$$

The plus or minus superscript denotes the total angular momentum, $j = \ell \pm 1/2$. The quantity $e^{2i\delta_\ell^\pm}$ is often called the scattering or collision function[30].

Due to the finite range, a, of the scattering potential, only the partial waves in the sum up to a maximum orbital angular momentum ℓ_{max} approximately equal to k•a, are strongly affected by the

Reproduced with permission of the copyright owner. Further reproduction prohibited without permission.

potential.

The contributions from the partial waves of higher angular momentum are very small or negligible. Since the incident energy of the neutron is large enough near the resonance to notice relativistic effects, the wave number, correct to first order, becomes:

$$k = \sqrt{\frac{2 m_1}{\hbar^2 \left[\frac{(1 + m_1/m_2)^2}{T} - \frac{(1 - \frac{m_1}{m_2})^2}{2 m_1 c^2} \right]}} \qquad 7$$

where m_1, is the rest mass of the neutron, m_2 is the rest mass of the alpha particle, $\hbar$ is Plank's constant divided by 2π , c is the speed of light and T is the laboratory kinetic energy of the incident particle.

If processes other than elastic scattering are possible, then the phase shift becomes complex. The real part of the phase shift represents the elastic scattering process and the imaginary part represents all other processes. If the phase shift is complex, the partial scattering amplitude becomes:

$$f_l^{\pm} = \frac{\eta_l^{\pm} \, e^{2 i \mu_l^{\pm}} - 1}{2 i} \qquad 8$$

where μ is the real part of the phase shift. The inelastic parameter, η , is equal to $e^{-2 \, \mathrm{Im} \, \delta}$.

The elastic scattering cross section, σ_{elas}, and the reaction cross section, σ_r, may be written in terms of the partial scattering amplitudes as[30]:

Reproduced with permission of the copyright owner. Further reproduction prohibited without permission.

$$\sigma_{elas} = \frac{\pi}{k^2} \sum_{j,l} (j + \tfrac{1}{2})\, 4\, |f_l^{\pm}|^2 \qquad 9$$

and

$$\sigma_r = \frac{\pi}{k^2} \sum_{j,l} (j + \tfrac{1}{2})\, 4 \left(I_m f_l^{\pm} - |f_l^{\pm}|^2 \right) \qquad 10$$

The total cross section, σ_t, is the sum of the elastic cross section and the reaction cross section. It may be written as:

$$\sigma_T = \frac{\pi}{k^2} \sum_{j,l} (j + \tfrac{1}{2})\, 4\, I_m f_l^{\pm} \qquad 11$$

In terms of the real part of the phase shift and inelastic parameter, equations 9, 10, and 11 may be rewritten as:

$$\sigma_{elas} = \frac{\pi}{k^2} \sum_{j,l} (j + \tfrac{1}{2}) \left[1 + (\tau_l^{\pm})^2 - 2\tau_l^{\pm} \cos 2\mu_l^{\pm} \right] \qquad 12$$

$$\sigma_r = \frac{\pi}{k^2} \sum_{j,l} (j + \tfrac{1}{2}) \left[1 - (\tau_l^{\pm})^2 \right] \qquad 13$$

$$\sigma_T = \frac{\pi}{k^2} \sum_{j,l} (j + \tfrac{1}{2}) \left[2 - 2\tau_l^{\pm} \cos 2\mu_l^{\pm} \right] \qquad 14$$

Assuming, on the basis of previous investigations[6,7,12,31] that the assignment of total angular momentum and parity of $3/2^+$ to be correct, the effects of the 16.7 MeV excited state is ^5He, as observed in the

Reproduced with permission of the copyright owner. Further reproduction prohibited without permission.

$n - \alpha$ scattering, should be contained in the $D_{3/2}$ phase shift and the f_2^- partial scattering amplitude. From single resonance theory[32], the f_2^- partial scattering amplitude in the vicinity of an isolated resonance may be written as:

$$f_2^- = \frac{e^{2i\phi_2^-} - 1}{2i} + G\left(\frac{e^{2i\beta} - 1}{2i}\right) e^{2i\phi_2^-} \qquad 15$$

where

$$G = \Gamma_n / (\Gamma_n + \Gamma_d) \qquad 16$$

Here, Γ_d and Γ_n are the partial widths for the decay into the deuteron + triton channel and the neutron + He^4 channel, respectively[+]. The resonant phase shift is designated as β ; ϕ_2^- is the non-resonant phase shift. The non-resonant phase shift contains contributions from distant levels, normally called potential scattering.

The resonant phase shift β is given as[34]:

$$\beta = \arctan\left[\frac{\frac{1}{2}(\Gamma_n + \Gamma_d)}{E_\lambda + \Delta_\lambda - E}\right] \qquad 17$$

where E_λ is the characteristic energy of the resonance, E is the

---

[+]The partial width Γ_γ , for the decay of the state to He^5 (ground state) + γ is negligibly small[33] and will not be considered.

Reproduced with permission of the copyright owner. Further reproduction prohibited without permission.

center-of-mass energy of the neutron and alpha particle and Δ_λ is the level shift.

The level shift[32] is defined as:

$$\Delta_\lambda = -(S_N - B_N)\gamma_N^2 - (S_d - B_d)\gamma_N^2 \qquad 18$$

where S_n and S_d are respectively the neutron and deuteron shift functions defined as

$$S = \left[\frac{kr}{2} \frac{d}{d(kr)} \ln \left(F_\ell^2 + G_\ell^2 \right) \right]_{r=a} \qquad 19$$

The symbols F_ℓ and G_ℓ represent the regular and irregular Coulomb wave function respectively. The terms B_n and B_d are arbitary constants picked such that at $E_\lambda = E$, $\Delta_\lambda = 0$ and therefore $\beta = 90°$.

The partial widths, Γ_n and Γ_d, may also be written in terms of the reduced widths as[34]:

$$\Gamma = 2\gamma P \qquad 20$$

where the penetrability, P, is defined as:

$$P = \left(\frac{kr}{F_\ell^2 + G_\ell^2} \right)_{r=a} \qquad 21$$

It is now possible to rewrite equation 15, applying equations 16 and 20, in terms of the reduced widths as:

Reproduced with permission of the copyright owner. Further reproduction prohibited without permission.

$$f_2^- = \frac{e^{2i\phi_2^-} - 1}{2i} + \frac{1}{1 + g\, P_d/P_N} \left(\frac{e^{2i\beta} - 1}{2i} \right) e^{2i\phi_2^-} \qquad 22$$

where $g = \gamma_d^2/\gamma_n^2$. 23

Thus the partial scattering amplitude, f_2^-, and in turn the phase shift, μ, τ, may be directly related to the reduced widths.

If the partial scattering amplitude as expressed in equation 8 is plotted in the complex plane, as in Figure III, it is found for example, that for constant τ, f_2^- traces out a circle of radius $\tau/2$ with a center, C, at (0, 1/2). If τ varies with energy a circular path is traced out inside the unitary circle--the unitary circle being the path scribed by f_2^- for $\tau = 1$. The angle between a line from the center of the circle (0, 1/2) and some point P on the circle is equal to 2μ. The phase shift, μ, varies from 0 through 180° if f_2^- passes above the center of the unitary circle. If the path passes beneath the center of the unitary circle, the phase shift increases to a value less than 90° and then decreases to zero, well above the resonance.

If f_2^- in the form of equation 15 is plotted in the unitary circle, (see Figure III) it becomes possible through elementary geometry to graphically determine the phase shift for the different nuclear parameters.

Reproduced with permission of the copyright owner. Further reproduction prohibited without permission.

RELATIONSHIP OF G, γ, β, ϕ, AND μ

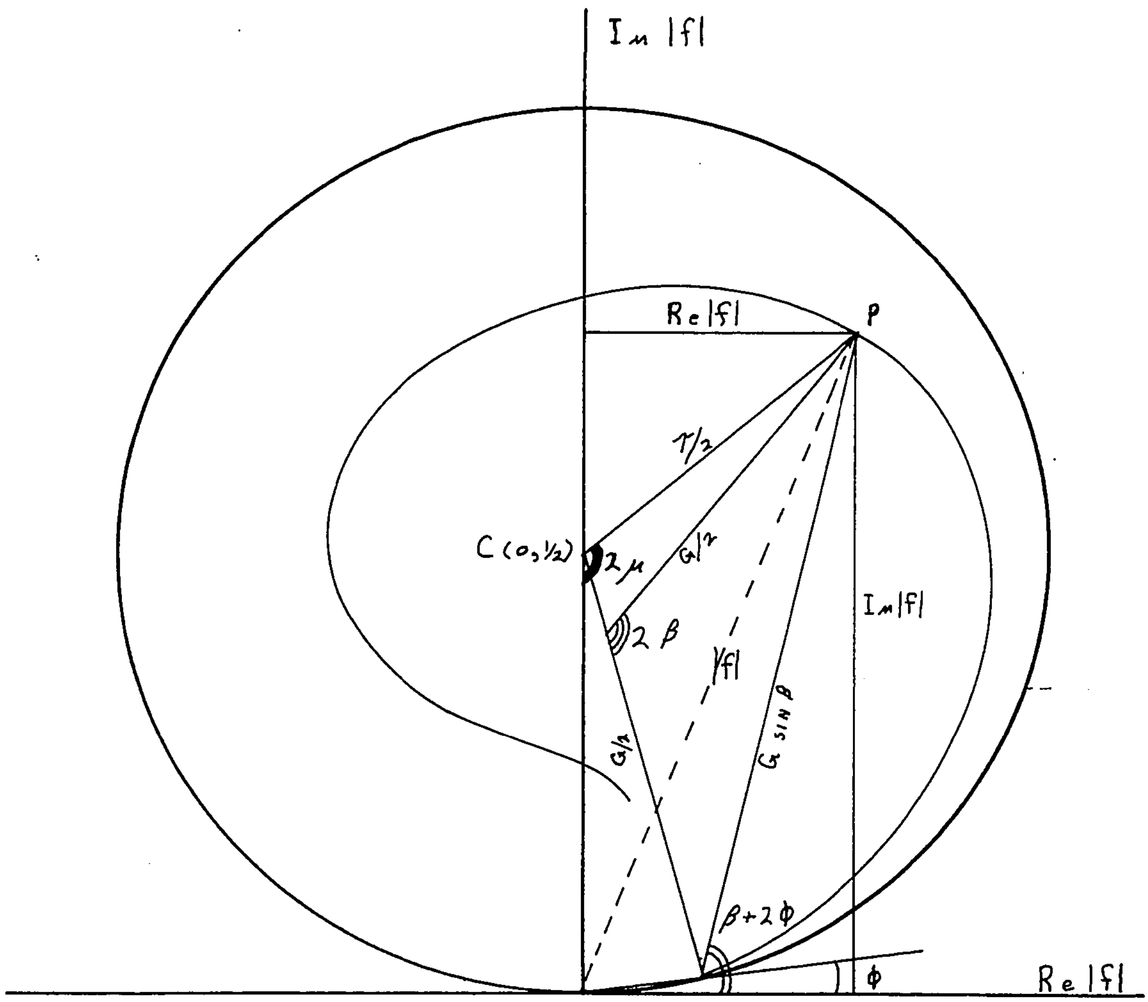

Figure III. Relationships between the real part of the phase shifts, μ, the inelastic parameter, γ, the resonant phase shifts, β, the potential phase shift, ϕ, and the partial scattering amplitude, f.

Reproduced with permission of the copyright owner. Further reproduction prohibited without permission.

CALCULATIONS

Qualitative Restrictions on $\mathrm{Im}|f_2^-|$ and $|f_2^-|$

It is useful to perform a qualitative examination of the cross sections. This may provide restrictions on the partial scattering amplitude and in turn on the nuclear parameters. If it can be assumed that the change in the cross sections near the resonance is due entirely to the $D_{3/2}$ state in ^5He, equations 9, 10 and 11 provide useful information on the path of f_2^- in the unitary circle.

The maximum imaginary component of f_2^- may be determined by evaluating the maximum change in the total cross section at the resonance. If the change in the total cross section is strictly due to the level in ^5He then an extrapolation from above and below the resonance should account for the contributions to the total cross section from the other levels. From the available data[20] the maximum change in the cross section is approximately 220 mb. and occurs at an incident neutron energy of 22.16 $\pm$ .01 MeV. From equation 11 the maximum imaginary component of f_2^- is found to be: $\mathrm{Im}\, f_{2\ max}^- \approx .60$.

With the aid of equation 9 and the same general procedure, the maximum value of f_2^- may be determined from the total elastic cross section. The total elastic cross section peaks at 22.15 $\pm$ .01 MeV with a maximum change of approximately 150 mb. From equation 9 the maximum value of the partial scattering amplitude is found to be: $f_{2\ max}^- \approx .64$.

Reproduced with permission of the copyright owner. Further reproduction prohibited without permission.

Calculation of Υ

The parameter Υ may obtained from the He^4 (n,d) T cross section data by using equation 13. However, available He^4 (n,d) T data[20] are only relative data. Consequently it is best to determine the reaction cross section from studies of the inverse reaction, i.e., T (d,n) He^4. This may be readily performed by applying the reciprocity relationship as explained in Evans[35].$^+$ The calculation is reproduced in Appendix A.

There are two principal sets of data, Argo et al.[12], and Conner et al.[6], available for determining the T (d,n) He^4 reaction cross section. The two sets of data are consistent to within their experimental uncertainties--Conner et al., have a 3% uncertainty, Argo et al., have a 10% uncertainty.

The values of the inelastic paramēter, Υ , were determined with the aid of reciprocity relationship, equation 13, and the average of the available data[6,12]. At 22.173 MeV, maximum peak of the reaction cross section, the average He^4 (n,d) T cross section is larger than $2\pi/k^2$. If there are no other contributions at this particular level, this implies Υ is imaginary. But, Υ must be real. Because the analysis has been restricted to a single level interpretation, the

---

$^+$The threshold of the d + T reaction was taken to be 22.07 MeV to agree with the calculations of Hoop and the measurements by Shămu et al. However, it was calculated to be 22.0638 MeV, relativistically correct, using the method outlined by Morrison[36] and a Q for the reaction from Lauritsen and Ajzenberg[37].

Reproduced with permission of the copyright owner. Further reproduction prohibited without permission.

average value of the reaction cross section at E = 22.172 MeV and adjacent energies were adjusted ~~by~~ .546%, a value within the experimental uncertainty, so that τ was real. The adjusted reaction cross section also peaked at 22.17 $\pm$ .01 MeV with a maximum of 91.6 mb. The values determined for the inelastic parameter, τ, are found in Table II.

Restrictions on the Nuclear Parameters

The minimum value of τ places an additional restriction on the partial scattering amplitude, f_2^-, and the nuclear parameters. Since τ is nearly zero at 22.17 $\pm$ .01 MeV, from equation 8 it is found that $f_2^- \simeq i/2$ at the resonance. From equation 15, f_2^- is pure imaginary when β = 90°, provided the potential phase shift of ϕ = 5° may be neglected for a qualitative study. Assuming the potential phase shift may be neglected, the partial scattering amplitude at β = 90° becomes:

$$f_2^- = \frac{i}{2} = \frac{\Gamma_n \, i}{\Gamma_n + \Gamma_d} = \frac{i}{1 + \frac{\gamma_d^2}{\gamma_n^2}\frac{P_d}{P_n}}$$

This suggests that $\Gamma_n \approx \Gamma_d$. If $\Gamma_n/\Gamma_d > 1$, the phase shift changes through 180° If $\Gamma_n/\Gamma_d < 1$, the phase shift will approach 90° and then decrease well above the resonance to values near 0°. Previous investigators[10,12,27] have attempted to determine if $\Gamma_n/\Gamma_d > 1$ or $\Gamma_n/\Gamma_d < 1$ at the resonance. Due to insufficient scattering data their studies have been inconclusive.

Since $\Gamma_n/\Gamma_d \approx 1$ at the resonance energy, one may obtain an estimate of the value of g, by evaluating the penetrabilities as

Reproduced with permission of the copyright owner. Further reproduction prohibited without permission.

suggested by Bloch et al.[38] and Willard et al.[34] and solving for the value of γ_d^2/γ_n^2 at the resonance. From this, it is learned that the value of g for $\Gamma_n/\Gamma_d \approx 1$ is g $\approx$ 38.

Determination of the $D_{3/2}$ Phase Shift

To determine the phase shift graphically above the deuteron + triton threshold for the different nuclear parameters the value of G must first be determined. Since G may be written using equations 16, 20 and 23 as:

$$G = \frac{1}{1 + \frac{\gamma_d^2 P_d}{\gamma_n^2 P_n}} = \frac{1}{1 + g\frac{P_d}{P_n}}$$

it is convenient to vary only the value g. The values of P_d may be determined from the tabulation by Block et al.[38] or from plots of Coulomb functions by Sharp et al.[39] The neutron penetrability, P_n, may be determined from the expression as given by Willard[34]. It should be noted that the relative angular momentum between the incident neutron and alpha particle is $\ell = 2$, and $\ell = 0$ between the triton and deuteron.

The values chosen for g, were: g = 36, because of Conner's success with this value[6]; g = 45, because of Balashko's success with both the ^{5}He and ^{5}Li systems and because of Weitkamp's success for ^{5}Li; and g = 70, due also to Weitkamp's[11] success with the state in ^{5}Li. The value of g = 40 was not selected because of the availability of Hoop's[10] calculations for this value. The value of g = 53 was not chosen because it was consistent with only one set of data. The phase shifts were then graphically determined using the method as outlined

Reproduced with permission of the copyright owner. Further reproduction prohibited without permission.

in Chapter II. The paths of f_2^- for the different parameters are shown in Figure IV.

For the ratio of g = 70, it was not possible to determine phase shifts above an incident neutron energy of E = 22.16 MeV using the above method. Above this energy, the experimental value of the reaction cross section was too large for a one level fit to the data. On the basis of existing data, it seems unlikely that other processes are contributing to the reaction cross section at this energy[27].

Below the deuteron + triton threshold, the partial scattering amplitude and in turn the phase shift were determined with the aid of equations 17, 18 and Figure III. In this energy range, the deuteron penetrability is zero. The deuteron shift function was determined from the Whittaker function as given by Lane and Thomas[32]. To calculate β, particular values of γ_n^2 and γ_d^2 must be chosen. To correspond with previous investigators[10,11], values of γ_d^2 of 1.5, 2.0 and 3.0 MeV were chosen. The values of γ_n^2 were then chosen such that $\gamma_n^2 = \gamma_d^2/g$, for the different values of g. The resonance energy was determined from the graphical determination of β above the deuteron + triton threshold. The quantity β was then calculated and plotted for each value of γ_d^2 and g. See Figures V, VI, VII. Due to the uncertainty in the graphical determination of β it was not possible to favor one value of γ_d^2 over another. Therefore, to be consistent with Weitkamp and Haeberli[11], $\gamma_d^2 = 1.5$ was used to determine the phase shift below the deuteron + triton threshold. See Table II for a tabulation of the phase shifts for the

Reproduced with permission of the copyright owner. Further reproduction prohibited without permission.

different parameters.

Calculations of the Cross Sections

Equations 1, 2, 3, 12, 13 and 14 lend themselves quite readily to analysis with a high speed digital computer. Following the procedure of Westin[40], a program was written in Fortran II for an IBM 1620 computer to evaluate the measured quantities as expressed in the above equations. A listing of the program may be found in Appendix C. The values used for the other phase shifts were those published by Hoop and Barschall[10]. For convenience, a tabulation of these values are included in Appendix A. Phase shifts for contributions from partial waves up through $\ell = 4$ were considered. An interaction radius of $r = 5.0 \times 10^{-13}$ cm. was used to include all nuclear interactions and to agree with previous investigators[6,10,11,27]. The results of these calculations were then compared with the experimental data.

Reproduced with permission of the copyright owner. Further reproduction prohibited without permission.

f_2^- IN THE COMPLEX PLANE

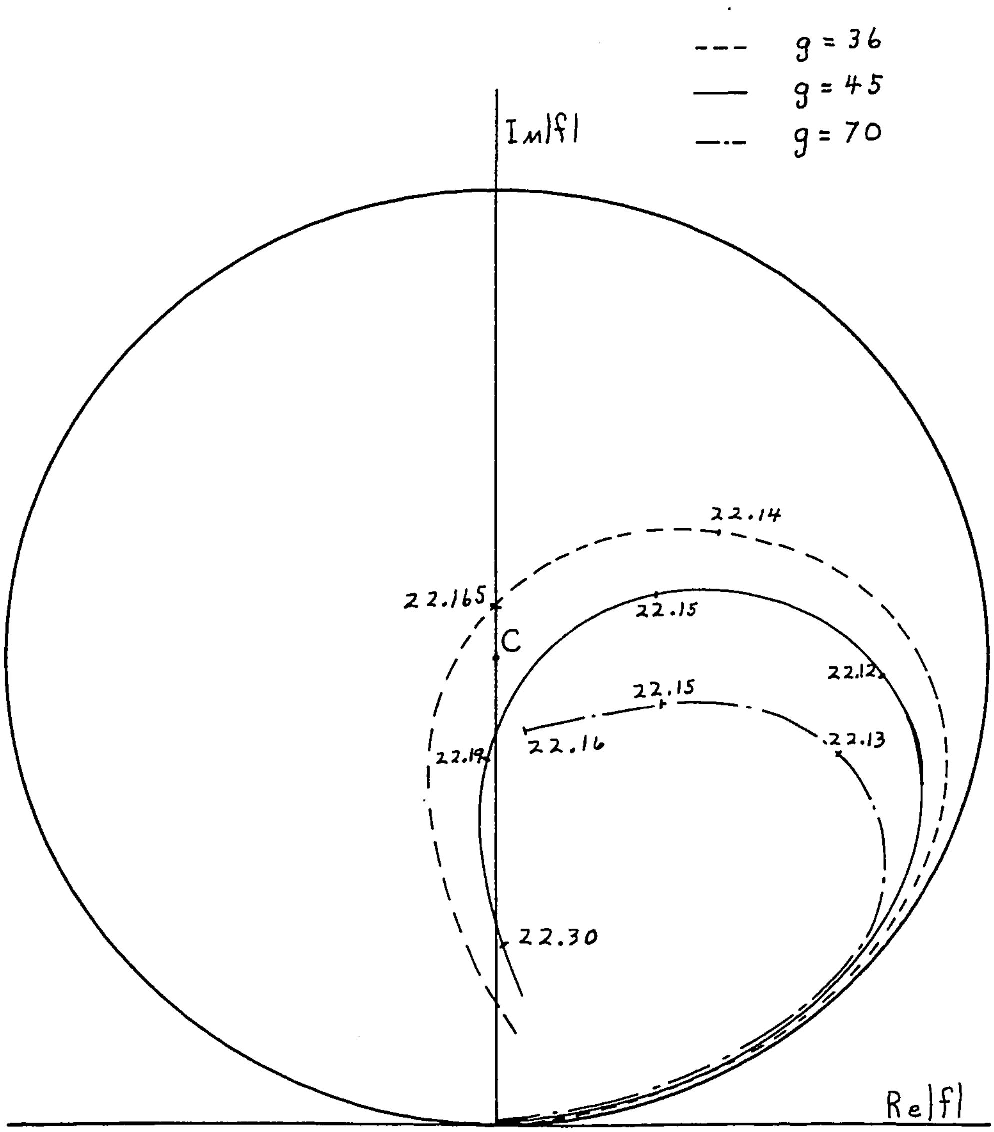

Figure IV. Behavior of the $D_{3/2}$ partial scattering amplitude, f_2^-, in the complex plane as a function of energy for the values of g = 36, 45 and 70.

Reproduced with permission of the copyright owner. Further reproduction prohibited without permission.

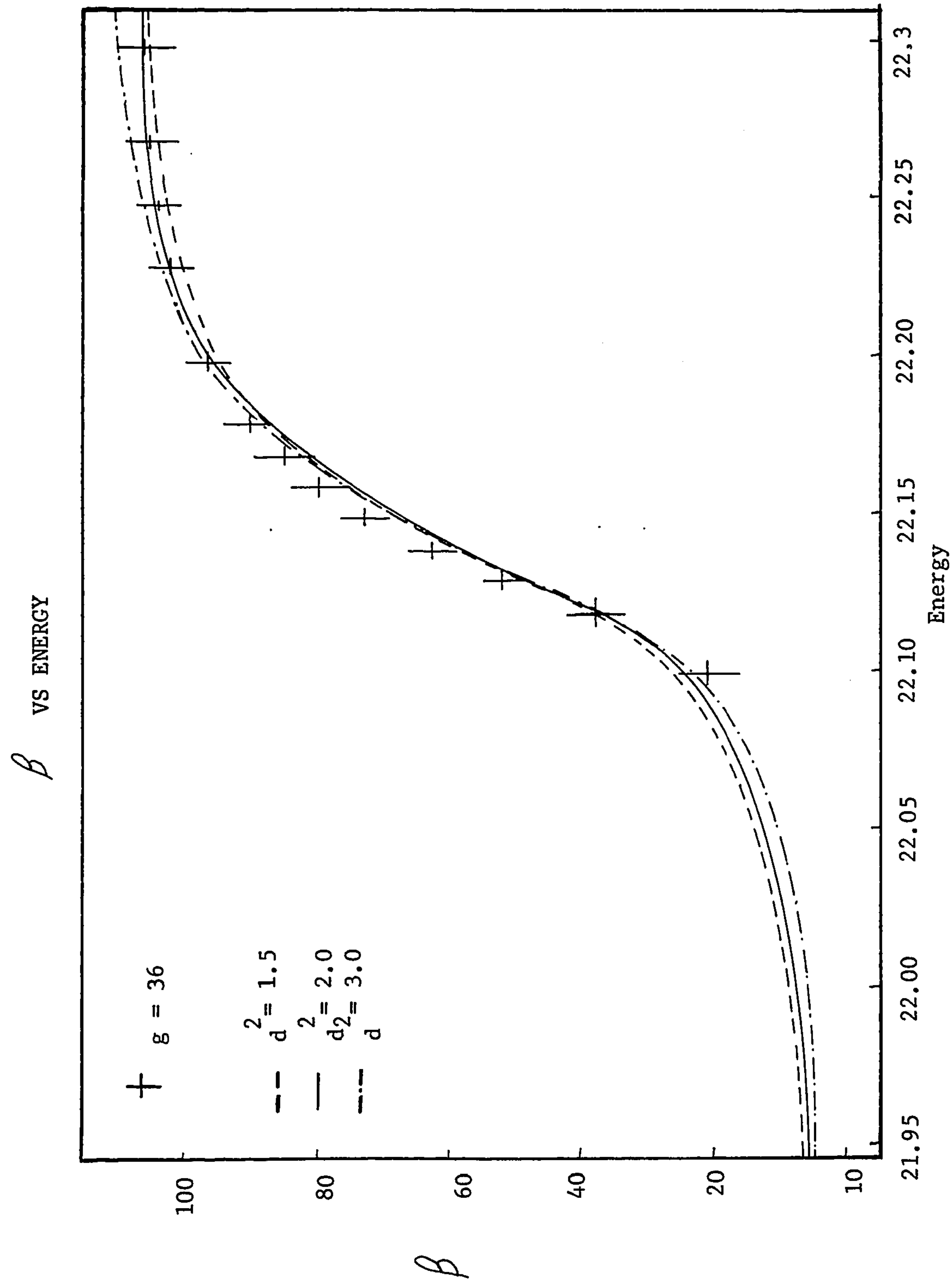

Figure V

Reproduced with permission of the copyright owner. Further reproduction prohibited without permission.

β VS ENERGY

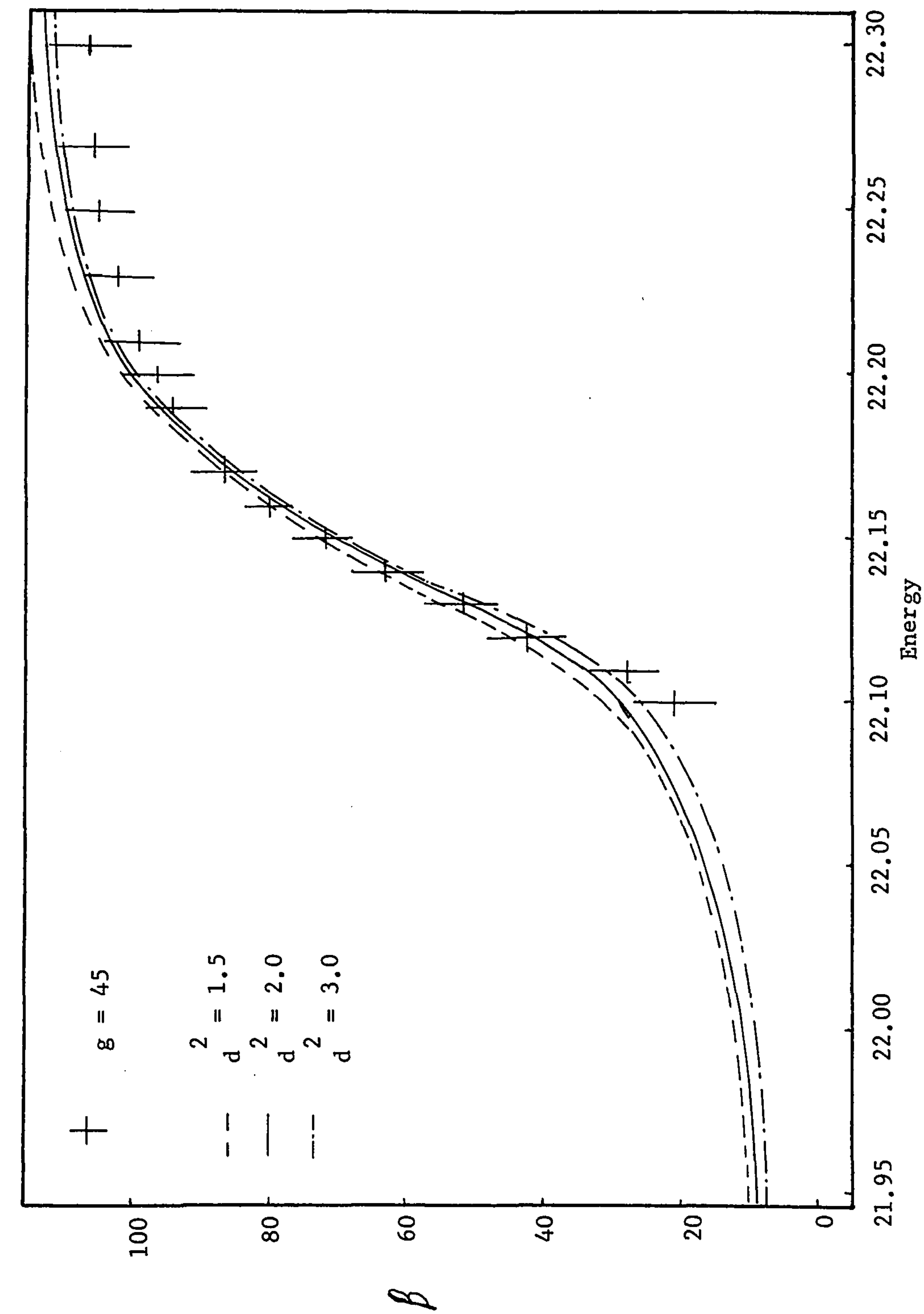

Figure VI

Reproduced with permission of the copyright owner. Further reproduction prohibited without permission.

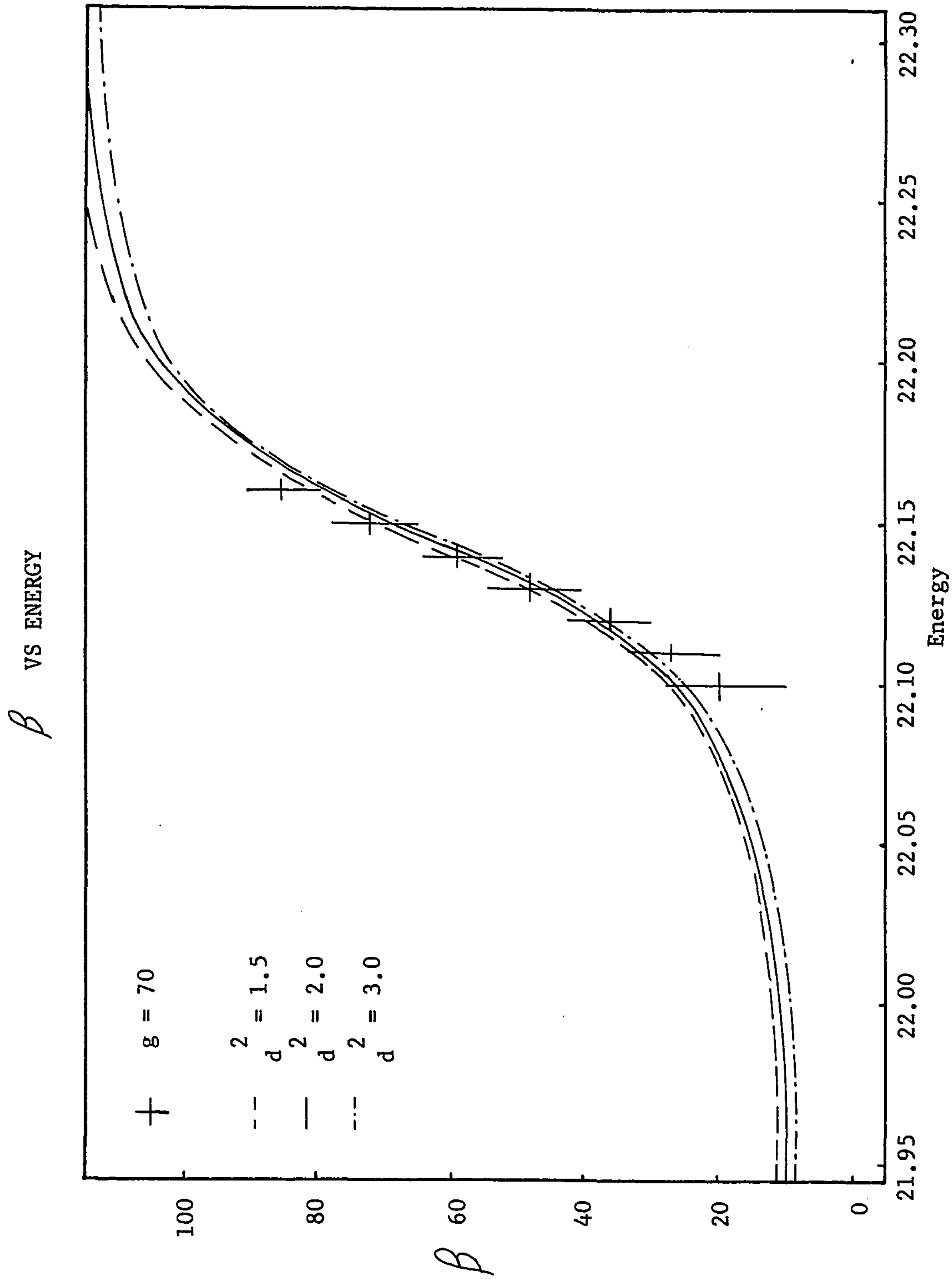

Figure VII

Reproduced with permission of the copyright owner. Further reproduction prohibited without permission.

Table II

$D_{3/2}$ Phase Shifts

Energy	τ_2^-	g = 36	g = 45	g = 70
21.85	1.000	11.75	11.75	11.75
21.90	1.000	13.00	12.00	12.26
22.00	1.000	16.25	15.50	15.40
22.05	1.000	20.05	19.00	18.25
22.09	.995	25.00	24.93	22.00
22.10	.980	28.00	27.50	23.50
22.11	.945	30.50	32.75	26.00
22.12	.844	43.00	40.00	31.50
22.13	.695	51.50	47.00	36.50
22.14	.530	60.50	51.50	38.00
22.15	.355	69.50	55.00	36.25
22.16	.175	79.25	54.00	10.00

Reproduced with permission of the copyright owner. Further reproduction prohibited without permission.

Table II Cont.

$D_{3/2}$ Phase Shifts

Energy	τ_2^-	g = 36	g = 45	g = 70
22.17	.060	112.00	25.00	
22.18	.100	145.00	5.00	
22.19	.190	157.50	-2.50	
22.20	.263	162.50	-3.50	
22.23	.416	169.25	-2.50	
22.26	.520	173.25	-1.00	
22.30	.615	177.00	-.01	
22.35	.679	178.70	1.00	
22.42	.700	179.68	3.20	
22.45	.715	180.25	4.00	
22.50	.732	181.25	5.50	
22.60	.748	181.50	7.40	

Reproduced with permission of the copyright owner. Further reproduction prohibited without permission.

COMPARISONS OF THE CALCULATIONS WITH THE DATA

Total Scattering Cross Section

Figures VIII and IX show the comparison of the data to the calculated total cross section curves for the different values of g. The error bars represent a 3% statistical uncertainty. The data have been corrected for a 40 kev energy spread in the incident beam.

The curve corresponding to g = 40 is calculated from the phase shifts published by Hoop and Barschall[10]. The agreement is improved if there is a relative shift between the data and Hoop and Barschall's calculation of seven kilovolts. A shift of seven kilovolts is within the uncertainty of the data. Rather than shift the data down, the calculation of Hoop and Barschall[10] was shifted up because no shift was necessary for the present calculation. This shift was performed for all of the following comparisons.

As was explained earlier, it was not possible using the experimental reaction cross section to determine phase shifts above 22.16 MeV for g = 70. Consequently, the total cross section for g = 70 is not plotted above this energy. The calculation for the ratio of g = 70 is not consistent with the data.

Comparing the calculated curves, it is found that varying the ratio of the reduced widths by 10%, has approximately a 2% effect in the maximum peak height. Consequently, the total scattering cross section is not unduly sensitive to small changes in the nuclear parameters.

Reproduced with permission of the copyright owner. Further reproduction prohibited without permission.

Figures VIII and IX. The data represent total neutron-alpha scattering over the $D_{3/2}$ resonance. The data have been corrected for a 40 kev energy spread in the incident beam. The incident neutron energy is in the laboratory system. The energy is measured in MeV; the cross section is measured in millibarns.

Reproduced with permission of the copyright owner. Further reproduction prohibited without permission.

TOTAL CROSS SECTION VS ENERGY

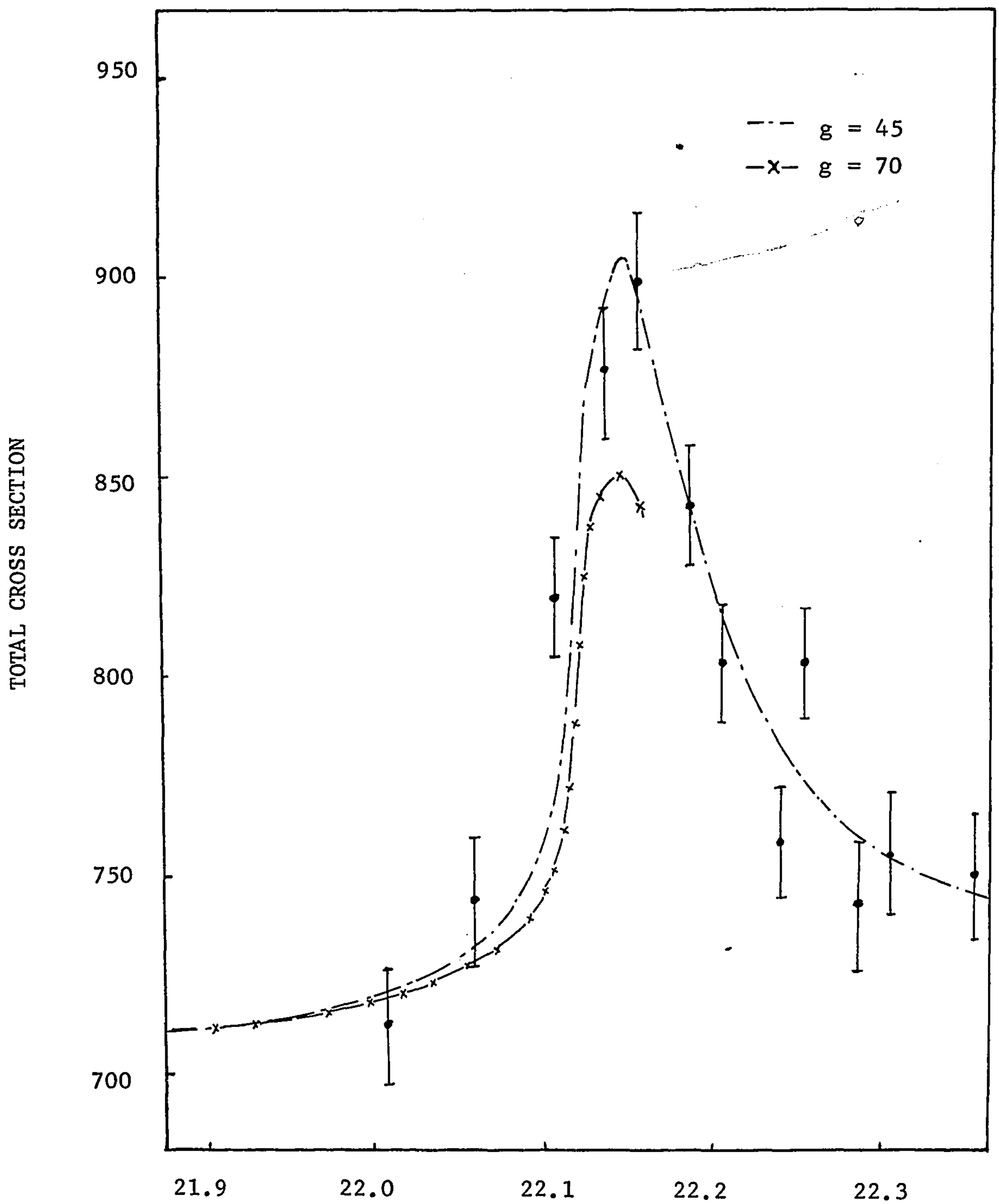

Figure VIII

Reproduced with permission of the copyright owner. Further reproduction prohibited without permission.

TOTAL CROSS SECTION VS ENERGY

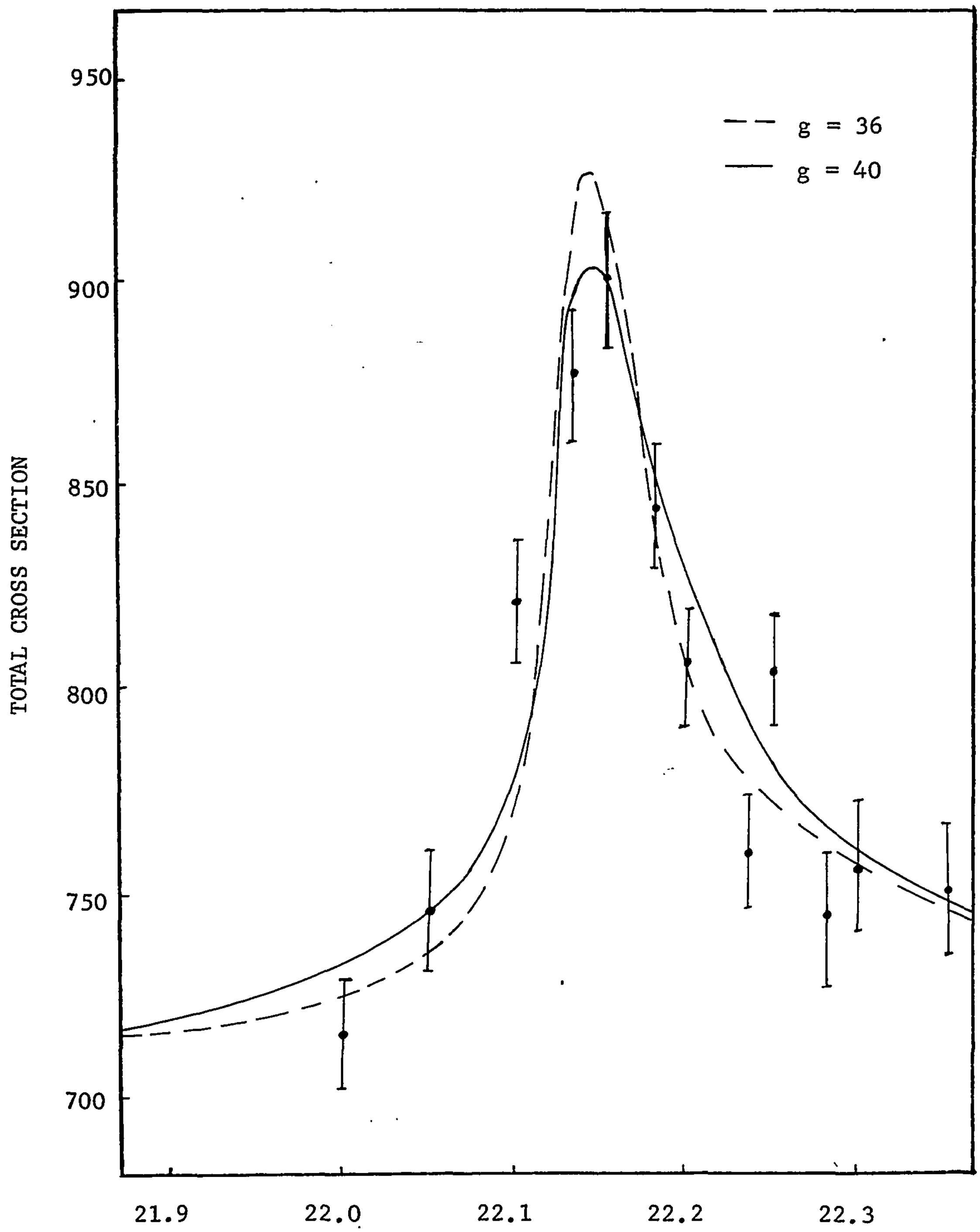

Figure IX

Reproduced with permission of the copyright owner. Further reproduction prohibited without permission.

Total Elastic Scattering Cross Section

Figures X and XI present the comparisons of the total elastic scattering cross section data to the calculations for the different parameters. The elastic scattering cross section was determined by subtracting the reaction cross section from the total cross section.

The ratios of g = 36, 40, 45 all provide reasonable fits with the data. The agreement for g = 70 is poor. Comparison of the calculated curves indicate that a change of approximately 10% produces a 2% change in the total elastic cross section at the peak of the resonance.

Differential Cross Section for Elastic Scattering as a Function of Energy

Data were available for the differential cross section as a function of energy at eight scattering angles[20]. The data have been normalized to the calculations of Hoop and Barschall[10] at 21.85 MeV. This normalization is consistent with that determined by comparing the differential cross section data, with the aid of a Legendre polynomial expansion[41,42], to the total elastic scattering cross section.

Comparisons have been made for all eight of these angles. The data for the angle of cos θ = .350 are felt to be uncertain for energies greater than 22.07 MeV incident neutron energy due to a possible error in the subtraction of the contribution from the

Reproduced with permission of the copyright owner. Further reproduction prohibited without permission.

Figures X and IX. Total Elastic Scattering Cross Section as a function of Incident Neutron Energy. The data represent the subtraction of the He^4 (n,d) T cross section from the total scattering cross section. The data have been corrected for a 40 kev energy spread in the incident beam. The error bars represent only the statistical uncertainty. The incident neutron energy is in the laboratory system. The energy is measured in MeV; the cross section is measured in millibarns.

Reproduced with permission of the copyright owner. Further reproduction prohibited without permission.

TOTAL ELASTIC CROSS SECTION VS ENERGY

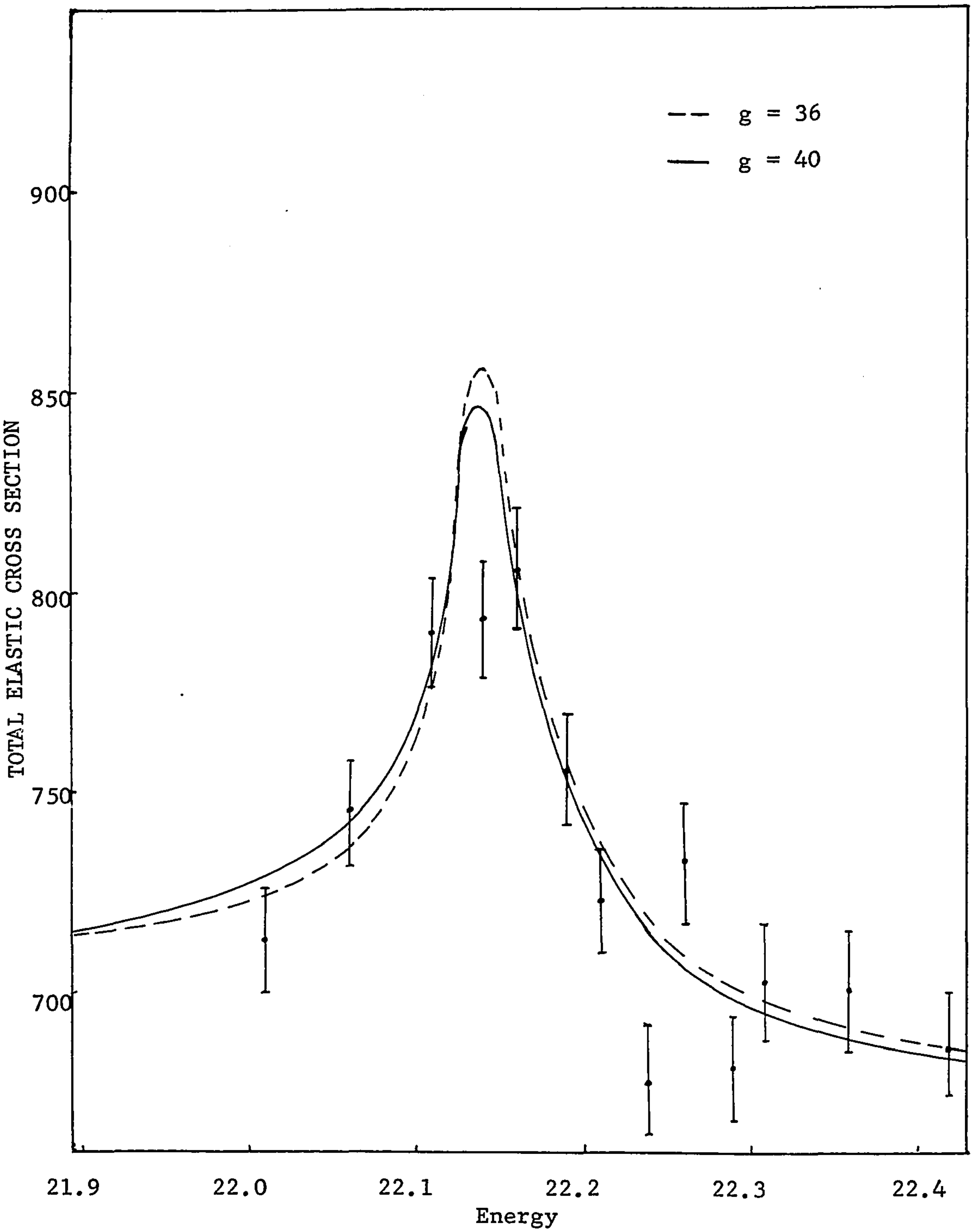

Figure XI

Reproduced with permission of the copyright owner. Further reproduction prohibited without permission.

TOTAL ELASTIC CROSS SECTION VS ENERGY

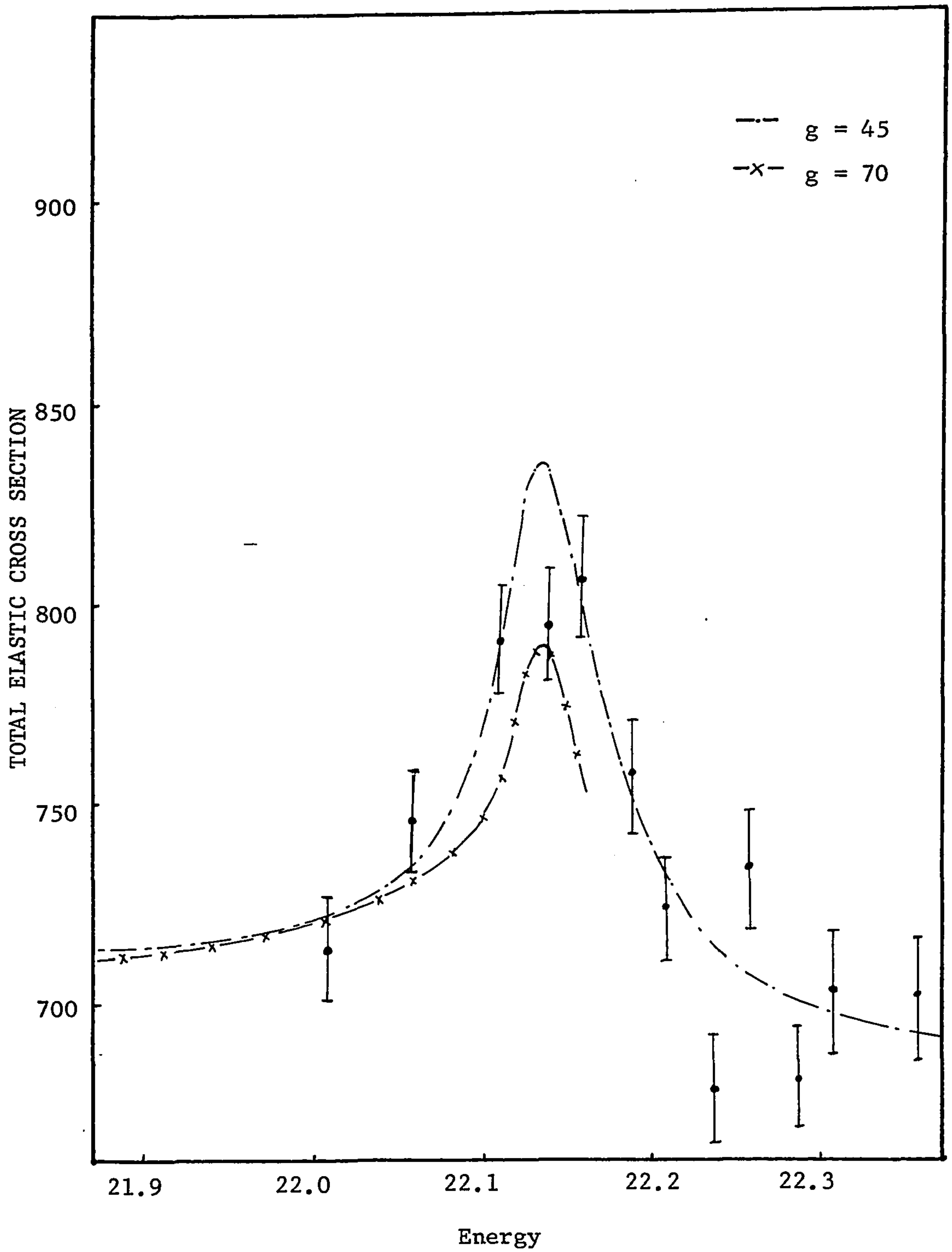

Figure X

Reproduced with permission of the copyright owner. Further reproduction prohibited without permission.

He^4 (n,d) T reaction. It was found that the experimental cross section at cos θ = .350 was not consistent with that obtained from the Legendre fit to the data at all angles. Since the Legendre fit must be consistent for all angles, one may conclude that the data for cos θ = .350 are in error. The cause of the discrepancy below an incident neutron energy of 22.1 MeV in the comparisons for cos θ = .126 and -.135 is not clear. It may be that too large of a correction was made for the background at these angles for energies less than the deuteron + triton threshold. Or, it may be that there is interference between the resonant and potential phases at the forward angles. It should also be noted that the Legendre fit is not consistent at these angles below the deuteron + triton threshold.

The curves corresponding to g = 40 were computed from the phase shifts published by Hoop and Barschall[13].

Comparisons for a ratio of g = 70 were not made since the phase shift could not be determined above 22.16 MeV.

Analysis of the curves indicates the ratio of g = 45 is favored over the ratios of g = 36 and g = 40. The ratio of g = 36 predicts a larger anomaly than the data indicate. It appears that this is a sensitive test, at the back scattering angles, of the value of g. A variation of 10% in the value of g produces a change from 1% to 10% in the peak height depending upon the scattering angle examined.

Reproduced with permission of the copyright owner. Further reproduction prohibited without permission.

Figures XII-XIX. Differential Cross Section vs Incident Neutron Energy. The data are relative data normalized to the calculation of Hoop and Barschall[10] at 21.85 MeV. The error bars represent a 10% error in the total background. The data have been corrected for a 70 kev energy spread in the incident beam. The incident neutron energy is in the laboratory. The energy is measured in MeV; the cross section is measured in millibarns.

Reproduced with permission of the copyright owner. Further reproduction prohibited without permission.

DIFFERENTIAL CROSS SECTION VS ENERGY

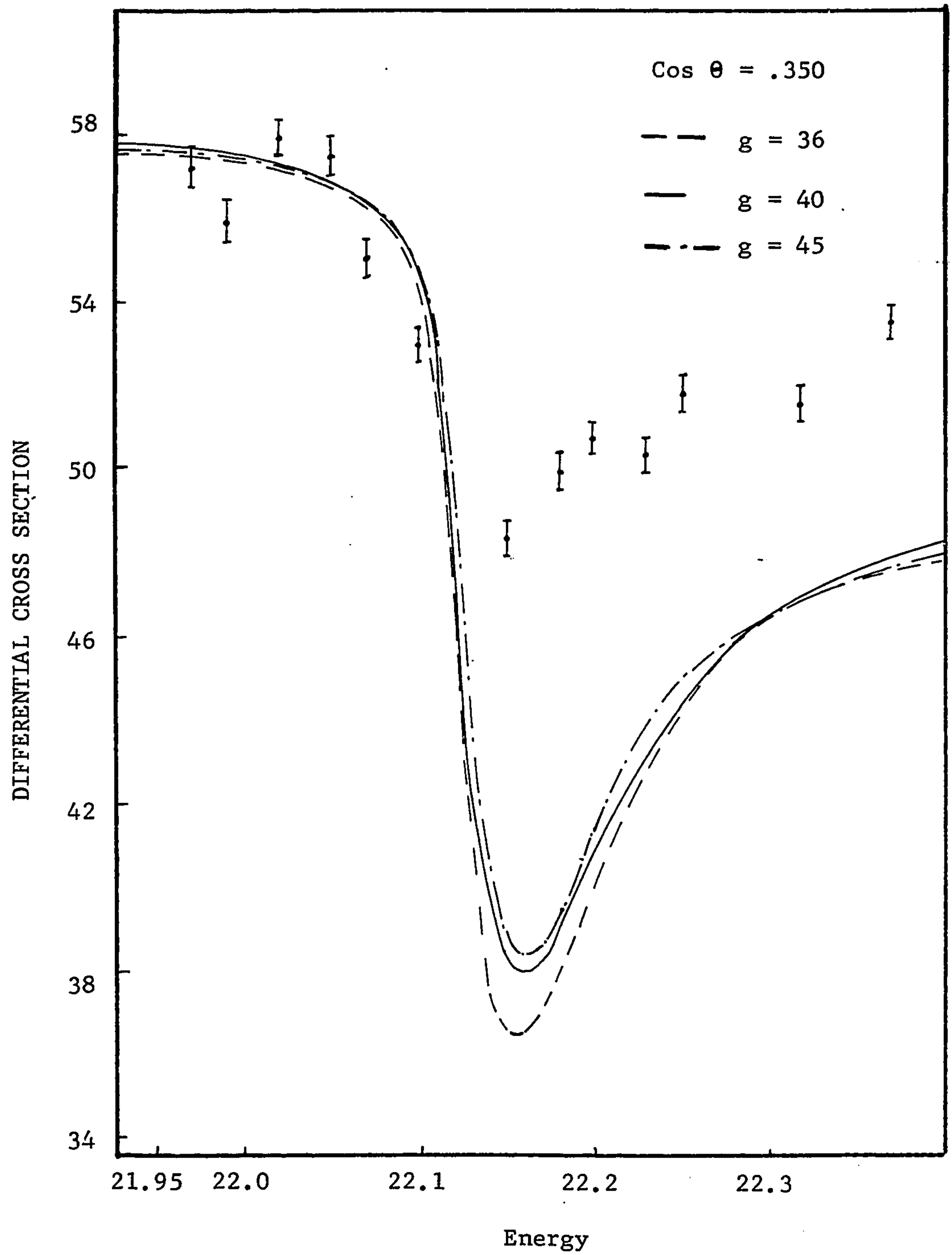

Figure XII

Reproduced with permission of the copyright owner. Further reproduction prohibited without permission.

DIFFERENTAIL CROSS SECTION VS ENERGY

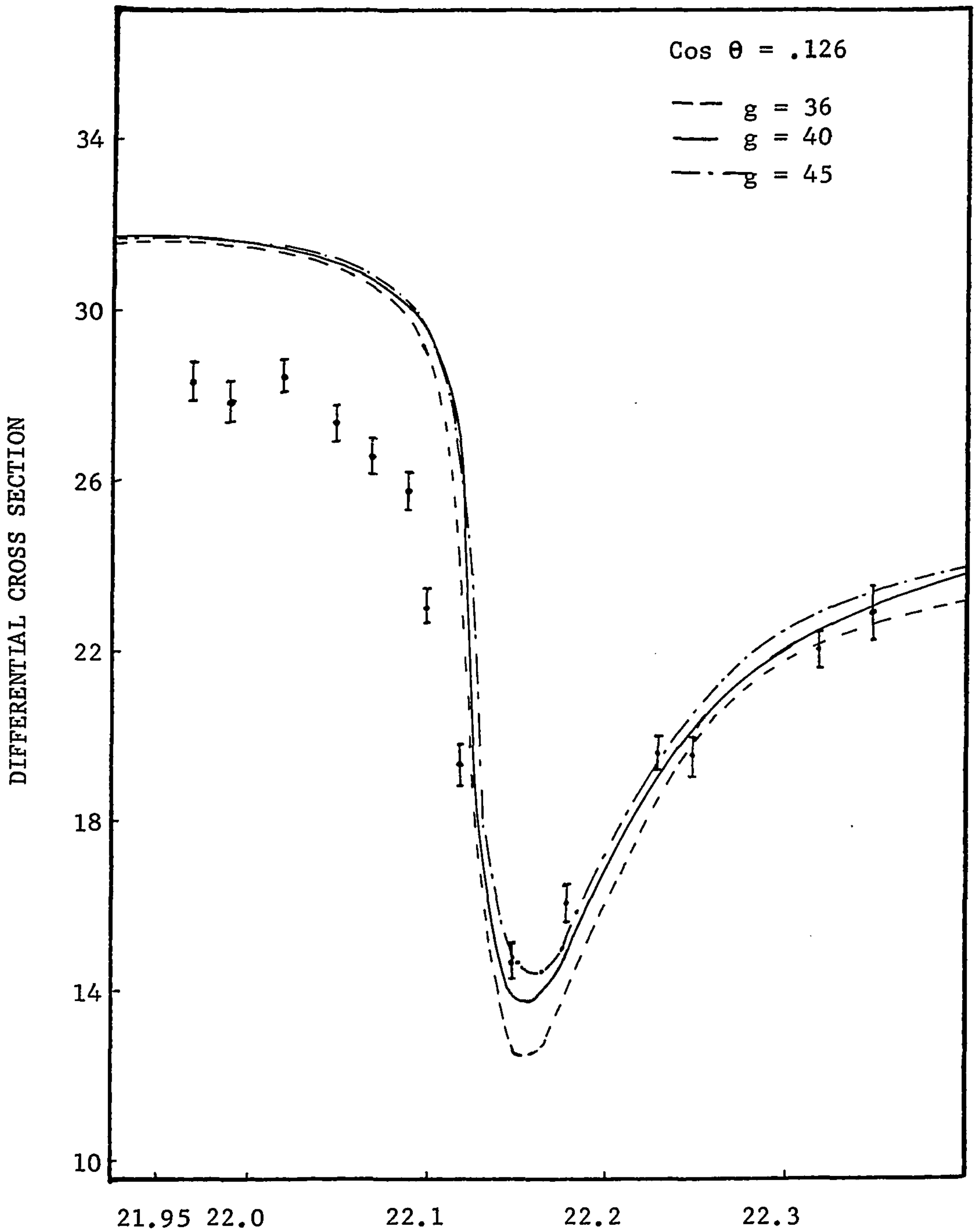

Figure XIII

Reproduced with permission of the copyright owner. Further reproduction prohibited without permission.

DIFFERENTIAL CROSS SECTION VS ENERGY

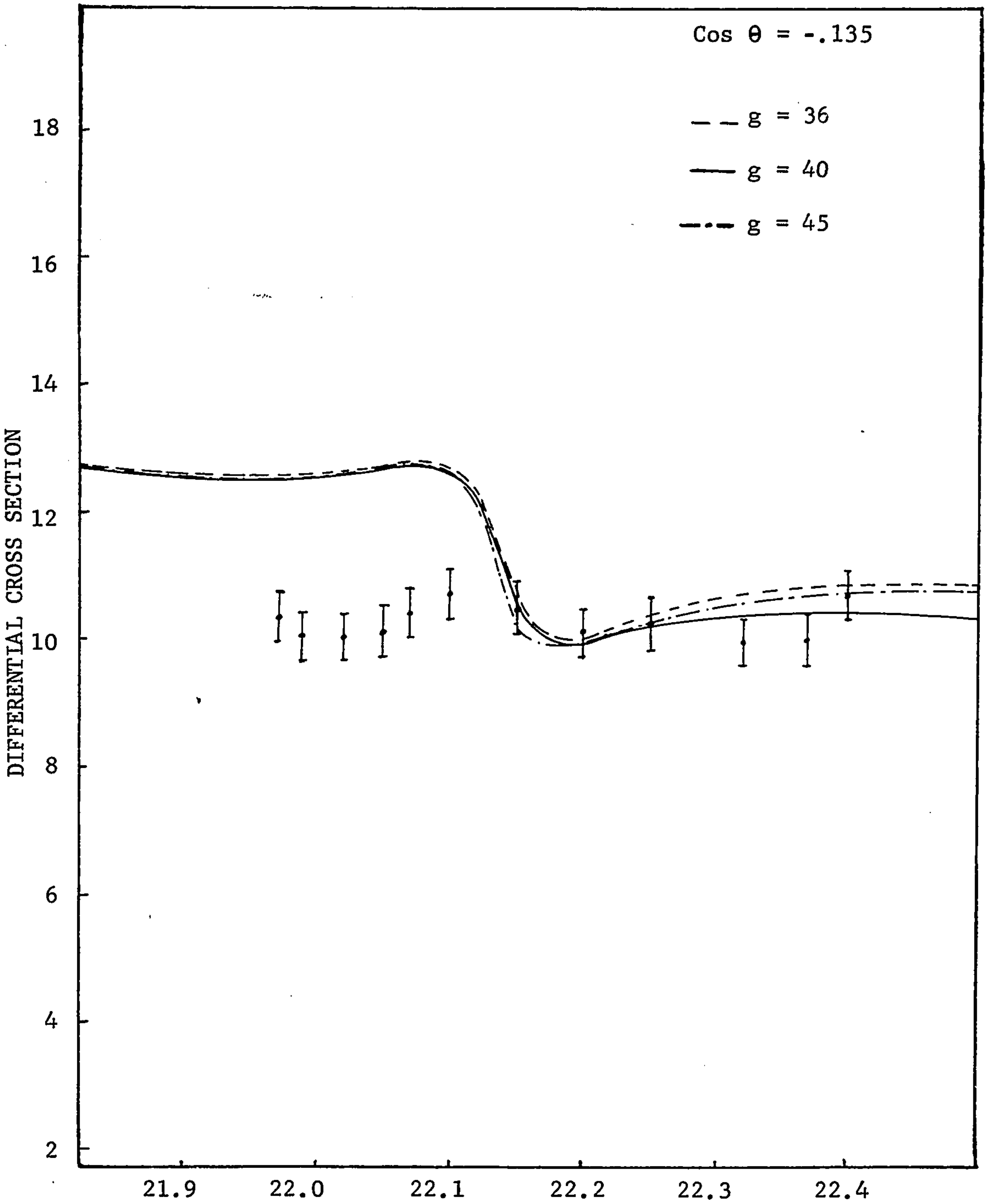

Figure XIV

Reproduced with permission of the copyright owner. Further reproduction prohibited without permission.

DIFFERENTIAL CROSS SECTION VS ENERGY

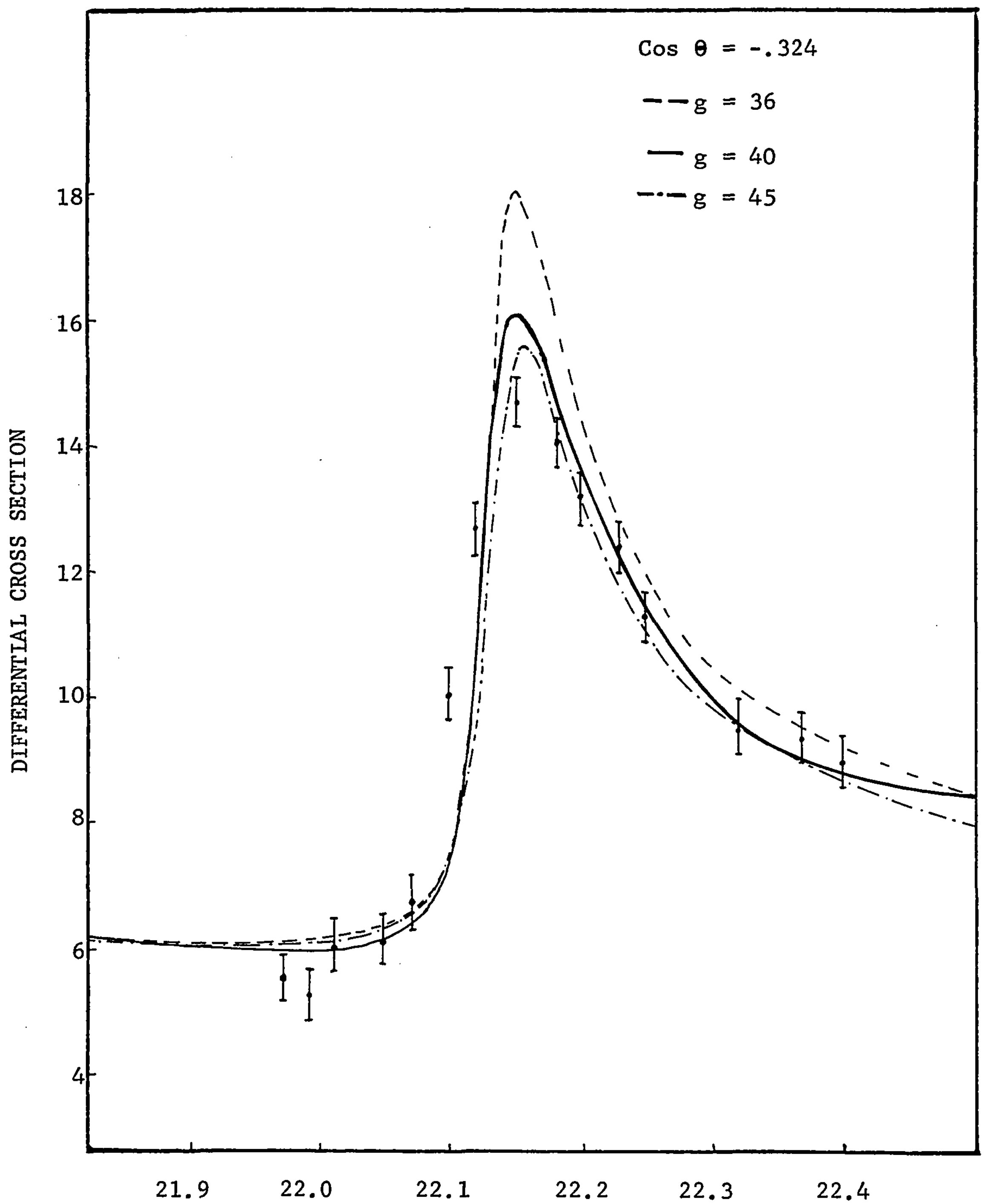

Figure XV

Reproduced with permission of the copyright owner. Further reproduction prohibited without permission.

DIFFERENTIAL CROSS SECTION VS ENERGY

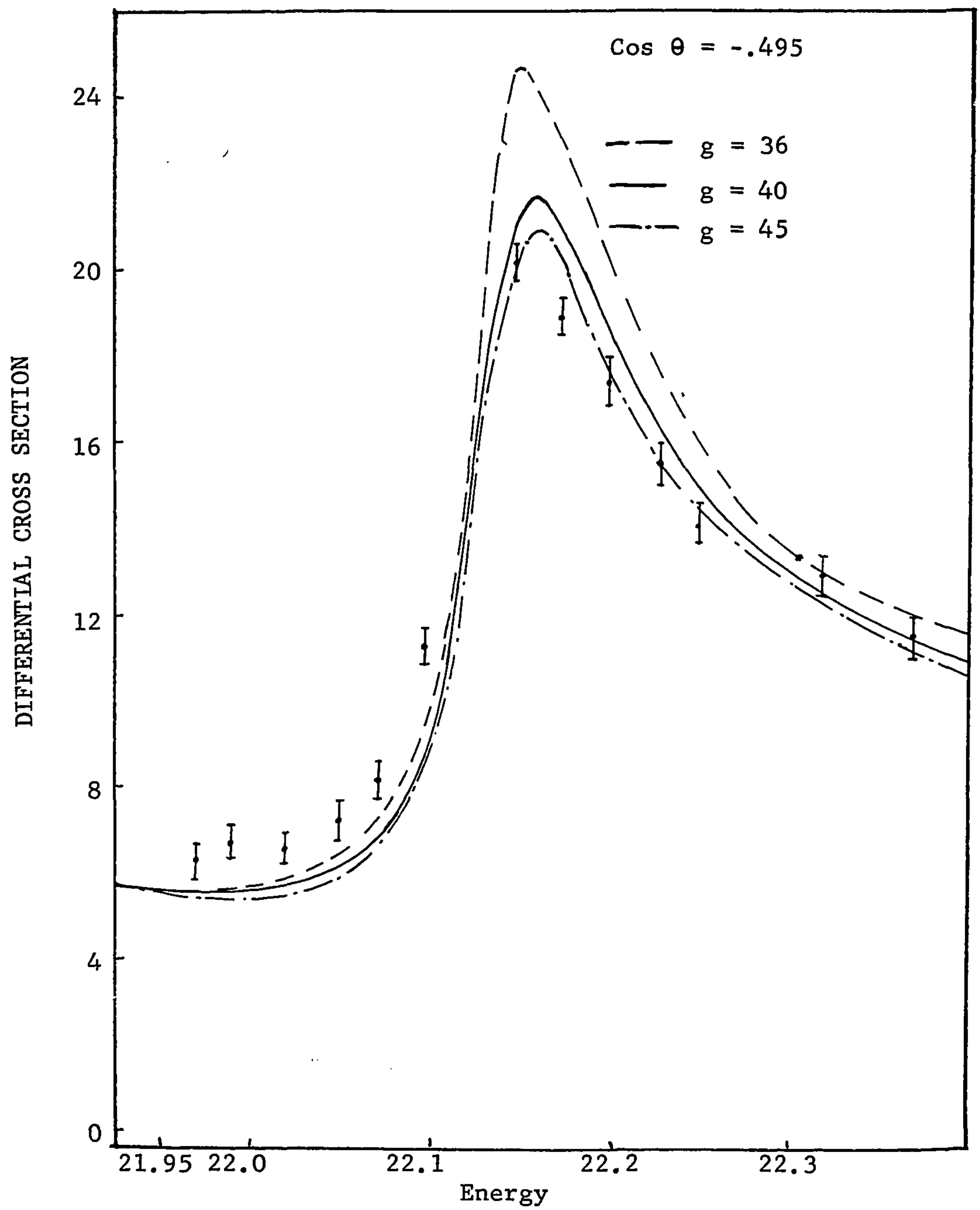

Figure XVI

Reproduced with permission of the copyright owner. Further reproduction prohibited without permission.

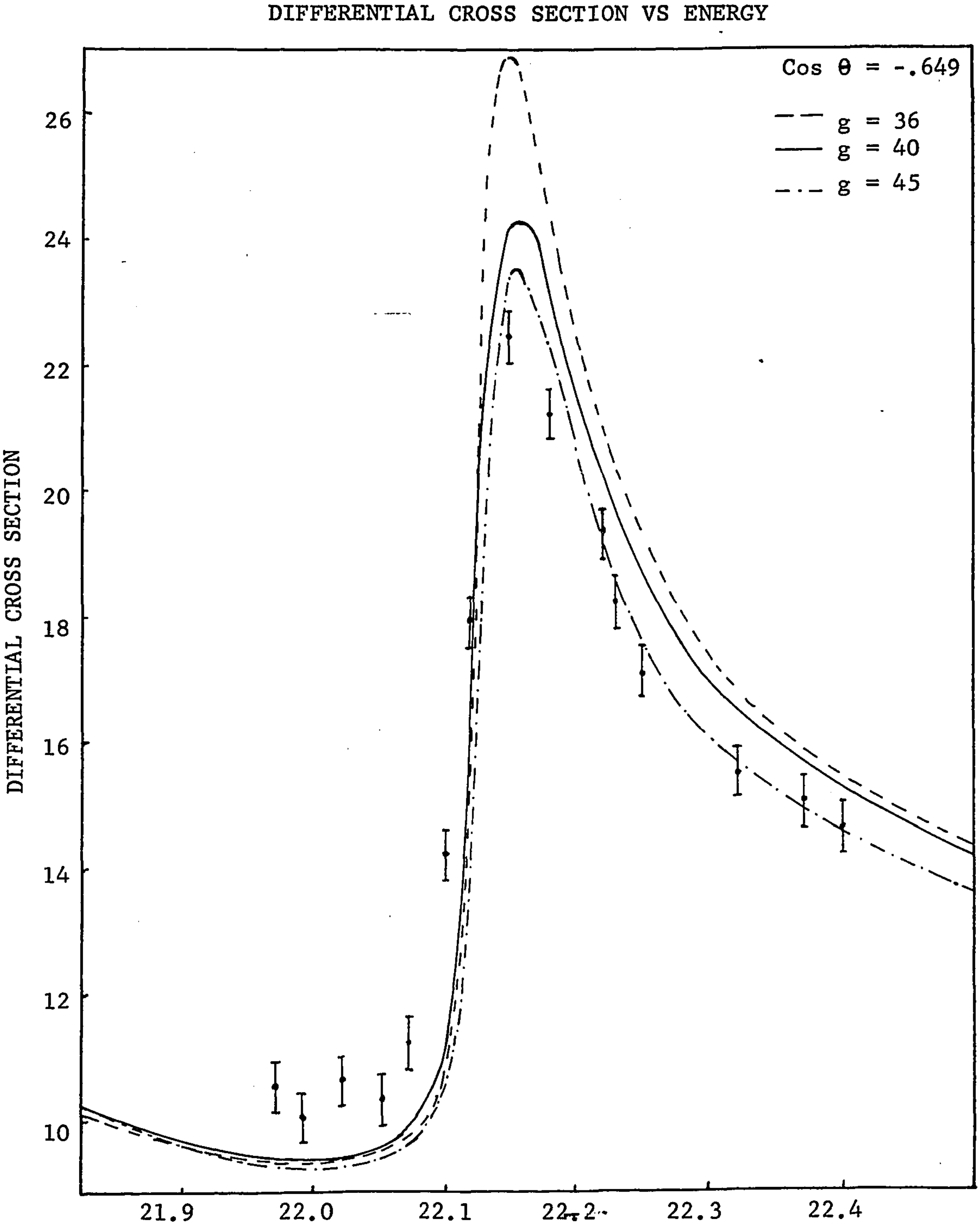

Figure XVII

Reproduced with permission of the copyright owner. Further reproduction prohibited without permission.

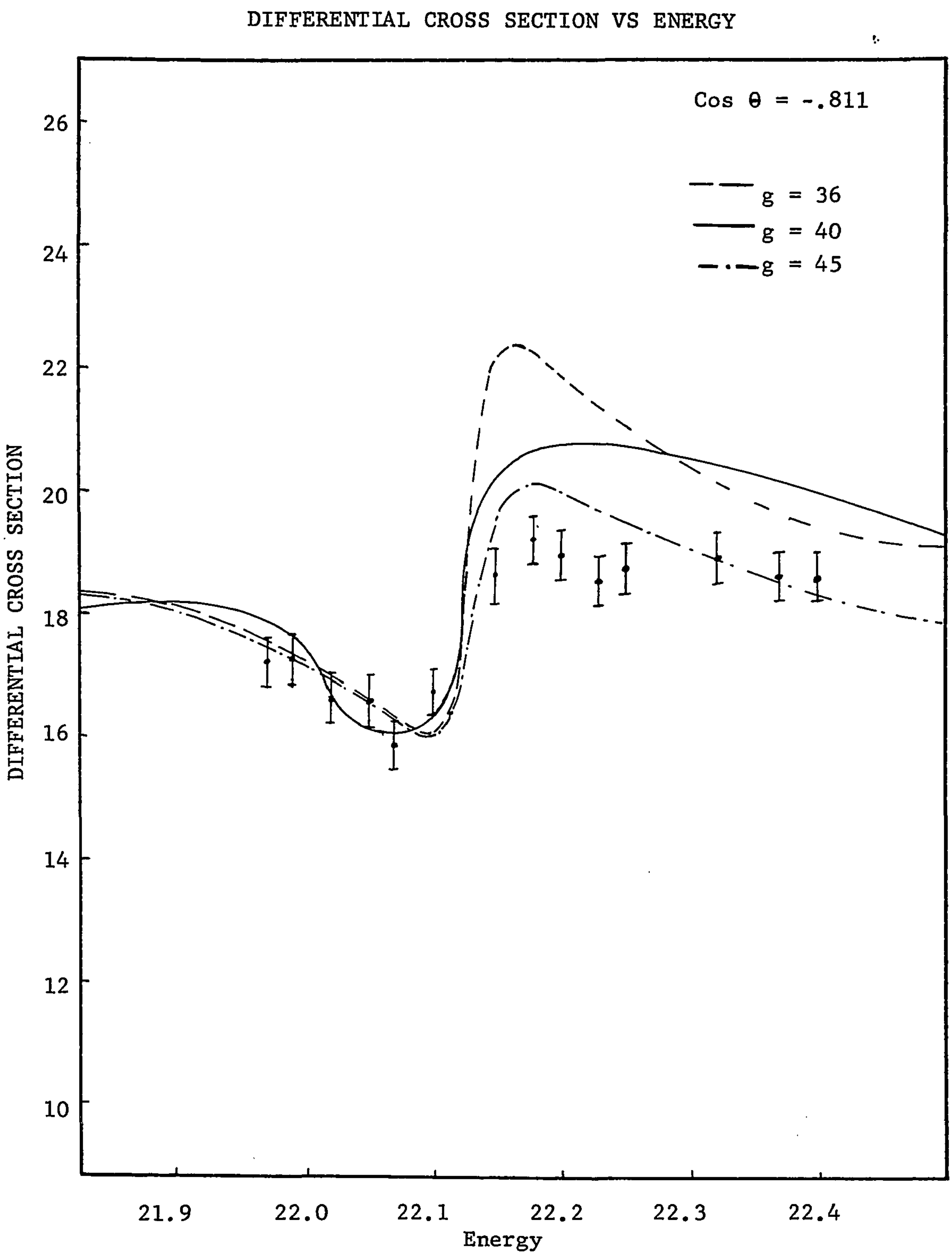

Figure XVIII

Reproduced with permission of the copyright owner. Further reproduction prohibited without permission.

DIFFERENTIAL CROSS SECTION VS ENERGY

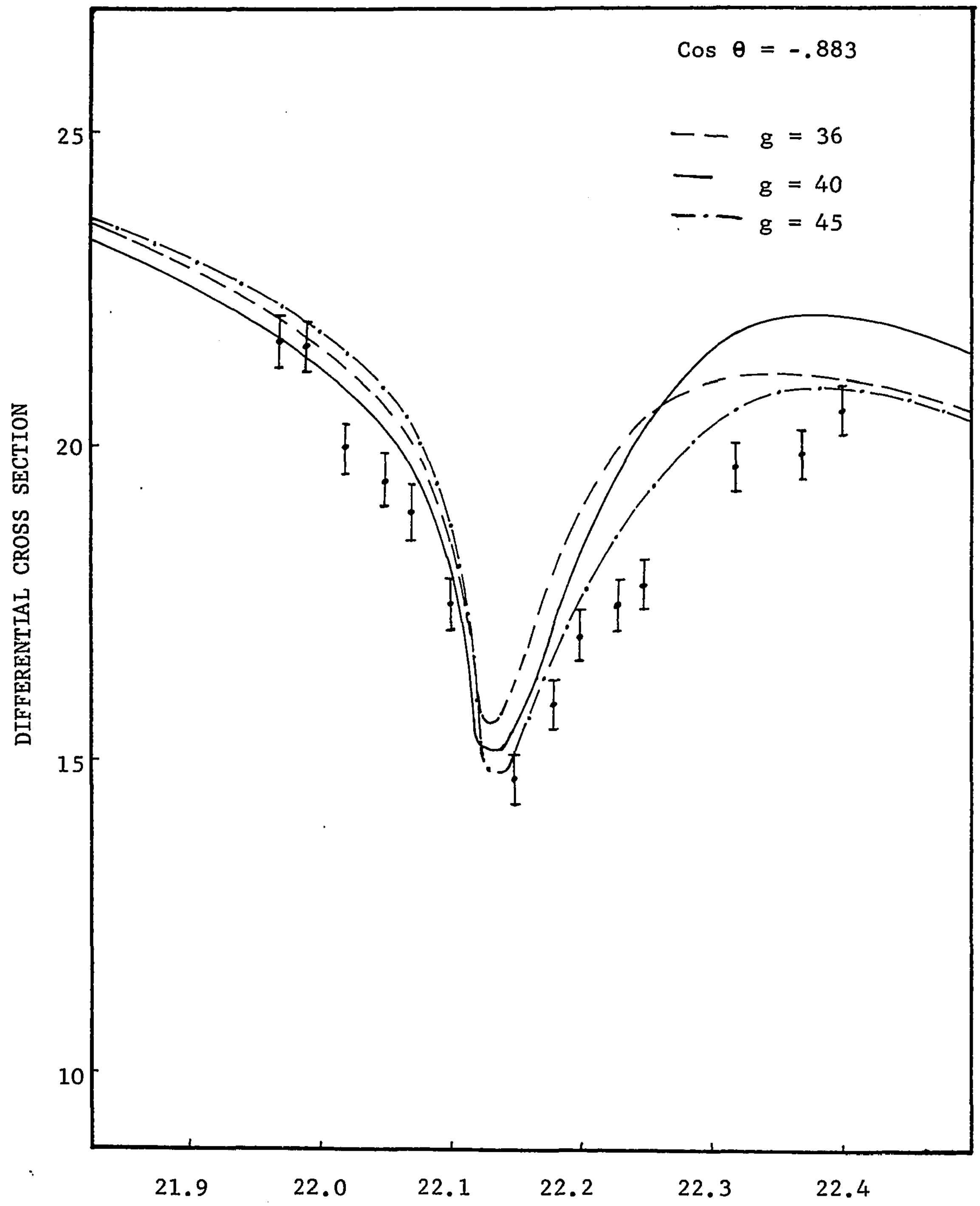

Figure XIX

Reproduced with permission of the copyright owner. Further reproduction prohibited without permission.

Differential Elastic Scattering Cross Section
as a Function of θ at 22.15 MeV

Figure XX shows a comparison of the differential cross section as a function of cos θ for incident neutron energy of 22.15 MeV. Here θ is the center-of-mass scattering angle. The data were relative data. The data were normalized in the same manner as described in the previous section. An analysis of the calculated curves indicates a change of approximately 10% in the value of g produces a maximum change in the differential cross section near cos θ = -.65 of 5%. At this energy the differential cross section is changing rapidly as a function of energy. If there is a slight shift in the energy scale, the sensitivity of this measurement could be exaggerated.

Examination reveals that the ratio of g = 45 produces an excellent fit to the data. The calculation for g = 40 produces a poor fit for angles near cos θ = 0. and near cos θ = -.6. The ratios of g = 36 and g = 70 certainly do not exhibit good fits. For g = 36 the discrepancy is approximately 19% at cos θ = -.6. For g = 70 the discrepancy is approximately 21% at cos θ = -.6. It should also be noted that a shift in energy of more than $\pm$ .03 MeV can not account for the discrepancy in agreement for the curves of g = 36, 40 or 70. A shift of this magnitude exceeds the uncertainty in the energy scale by a factor of three.

A peak appears in the differential cross section data between values of cos θ = .2 and cos θ = .45 due to deuteron + triton

Reproduced with permission of the copyright owner. Further reproduction prohibited without permission.

Figure XX. Differential Elastic Cross Section vs Cos θ at 22.15 MeV. The relative data were normalized to calculations of Hoop and Barschall[10] at 22.85 MeV. The data have been corrected for a 70 kev energy spread in the incident beam. The error bars represent a possible 10% error in the total background. The error due to the angular resolution is less than the error bars. The angle, θ, is the center-of-mass scattering angle. The incident neutron energy is measured in the laboratory system. The energy is measured in MeV; the cross section is measured in millibarns.

Reproduced with permission of the copyright owner. Further reproduction prohibited without permission.

DIFFERENTIAL CROSS SECTION VS COS θ

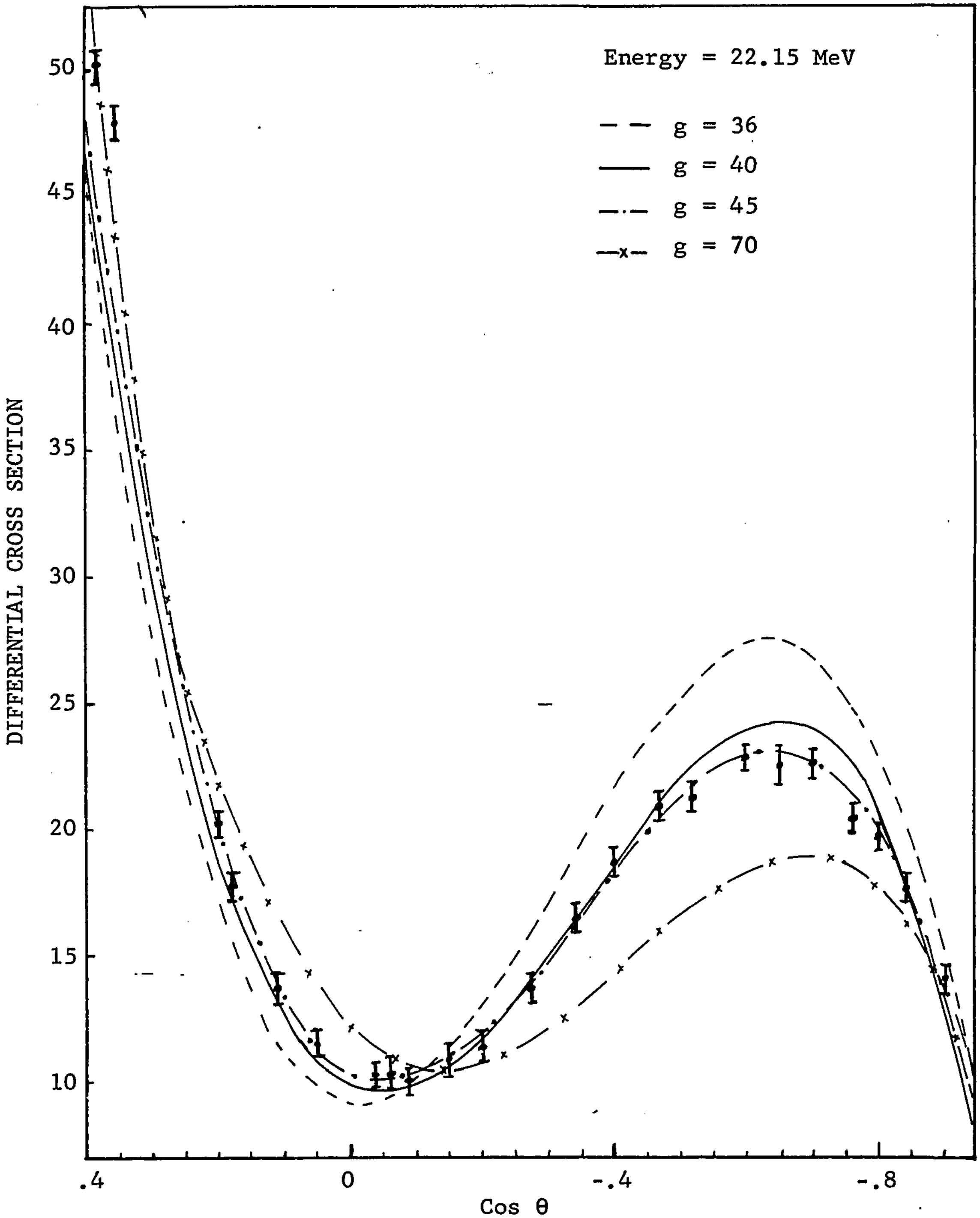

Figure XX

Reproduced with permission of the copyright owner. Further reproduction prohibited without permission.

reaction[44]. Because of this large background, the data point in this region have a large uncertainty. It is believed that this uncertainty accounts for the data point at angles of cos θ = .36 and cos θ = .38 lying above the theoretical curve.

Polarization Zero Crossing Angle

Figure XXI presents a plot of zero polarization crossing angle as a function of incident neutron energy. The data point[43] has not been corrected for all possible sources of error. The error bars given correspond to the possible zero-cross angle based on linear interpolation of relative asymmetries taken at ten degree intervals in the laboratory system[43]. The uncertainty in the energy scale is not known. The point has not been corrected for an energy spread in the incident beam.

The zero-cross angle does not appear highly dependent upon the ratio of the reduced widths. To differentiate between the ratios, the measurement would need to be accurate to within 2% over the resonance.

The discrepancy between the calculation of Hoop and Barschall[10] and the present calculations is due to Hoop and Barschall's choice of γ_d^2 = 2.0 MeV as compared to γ_d^2 = 1.5 MeV for the present analysis.

Reproduced with permission of the copyright owner. Further reproduction prohibited without permission.

Figure XXI. Polarization Zero Cross Angle vs Energy. The angle θ is the center-of-mass angle of zero polarization. The incident neutron energy is in the laboratory system.

Reproduced with permission of the copyright owner. Further reproduction prohibited without permission.

POLARIZATION ZERO-CROSS ANGLE VS ENERGY

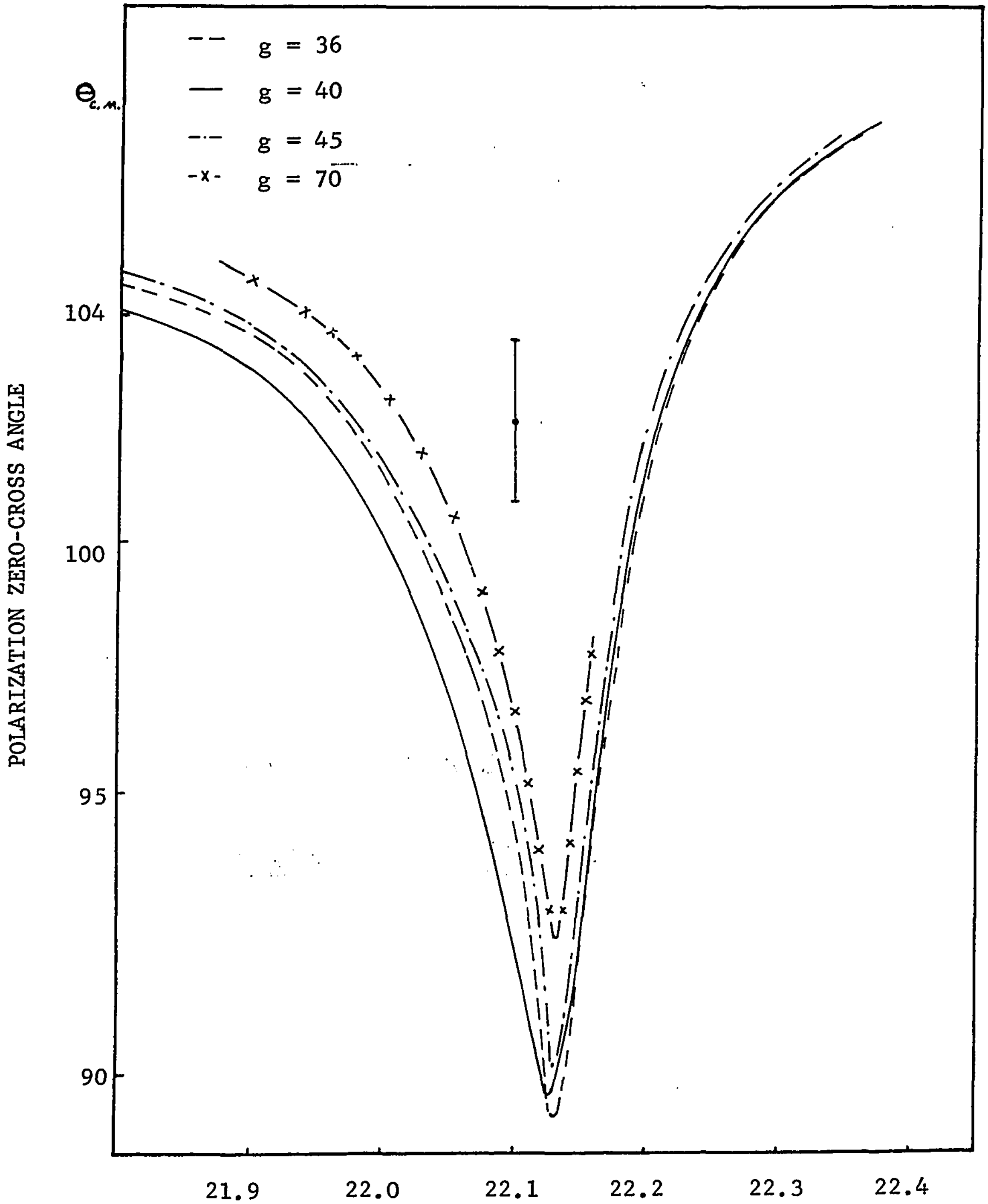

Figure XXI

Reproduced with permission of the copyright owner. Further reproduction prohibited without permission.

ANGLE OF ROTATION OF SPIN AND THE POLARIZATION

Angle of Rotation of Spin

Experimental data for the angle of rotation of spin over the resonance are also unavailable. Figures XXII and XXIII show a comparison of the calculated curves for the different values of g. The curves illustrated represent the angles at which the change over the resonance is maximum.

The discrepancy between the calculation of Hoop and Barschall[10] and the present analysis below the threshold may be attributed to Hoop and Barschall's choice of $\gamma_d^2 = 2.0$ MeV as compared to $\gamma_d^2 = 1.5$ for the present analysis.

Examination of the Polarization

Figures XXIV and XXV present the polarization as a function of the incident neutron energy in the region of the anomaly. Unfortunately, experimental data are not available over the resonance. Data are available at 21.1 MeV and 23.1 MeV. These have previously been compared by Hoop and Barschall[10].

The plots illustrated are for the angles which present the maximum change and maximum per centage change in the peak of the polarization. Comparison of the curves indicates that this is not a sensitive test for ratio of the nuclear parameters. A polarization experiment would need to be accurate to within 2% over the resonance to differentiate which of the ratios, g = 36, 40 or 45 is favored.

Reproduced with permission of the copyright owner. Further reproduction prohibited without permission.

Examination reveals that this measurement is not unduly sensitive to the different nuclear parameters. To differentiate which ratio is favored, measured data would need to have an uncertainty of less than 1% over the resonance.

Reproduced with permission of the copyright owner. Further reproduction prohibited without permission.

ANGLE OF ROTATION OF SPIN VS E

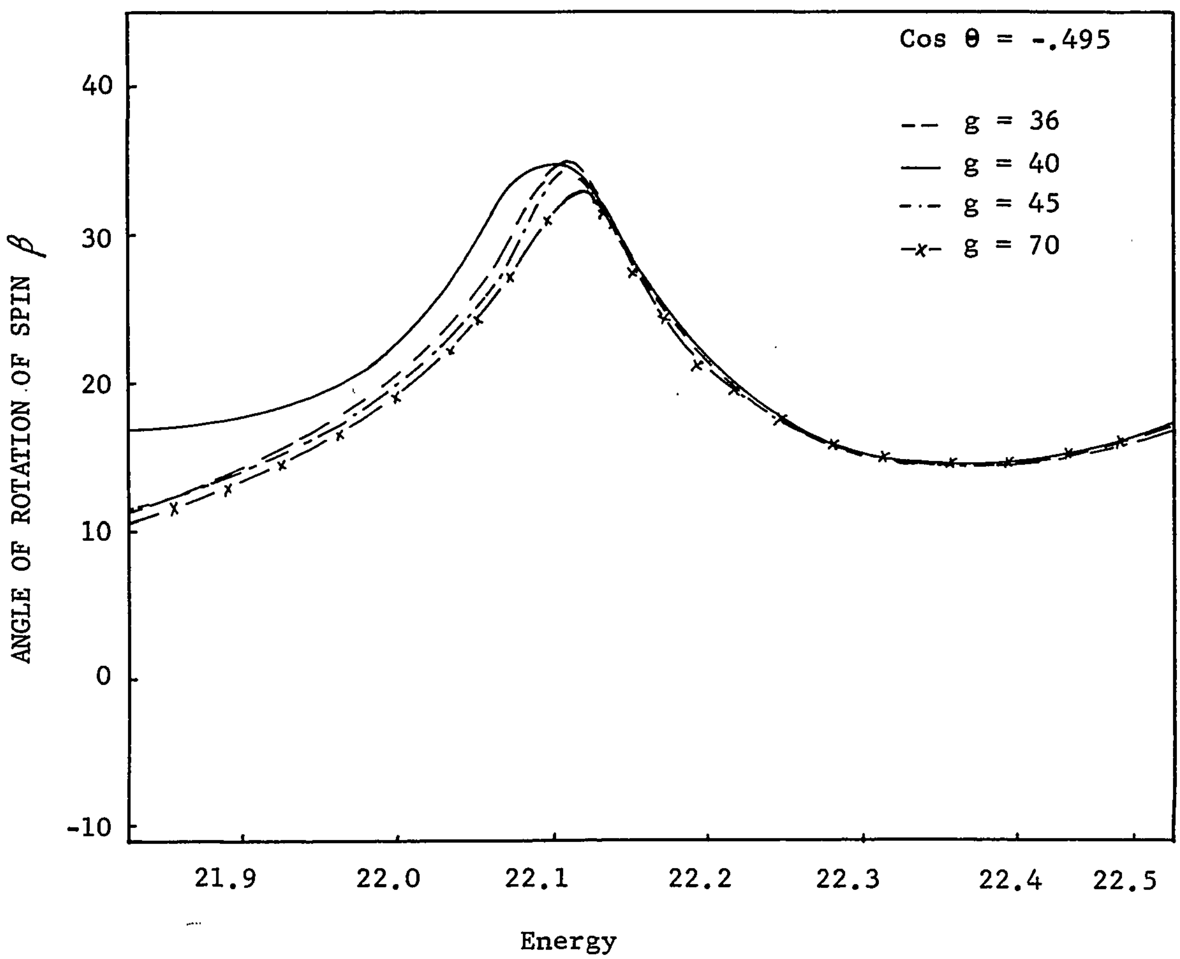

Figure XXII. Angle of Rotation of Spin vs the Incident Neutron Energy. The angle β is in the center-of-mass system. The incident neutron energy is in the laboratory system.

Reproduced with permission of the copyright owner. Further reproduction prohibited without permission.

ANGLE OF ROTATION OF SPIN VS ENERGY

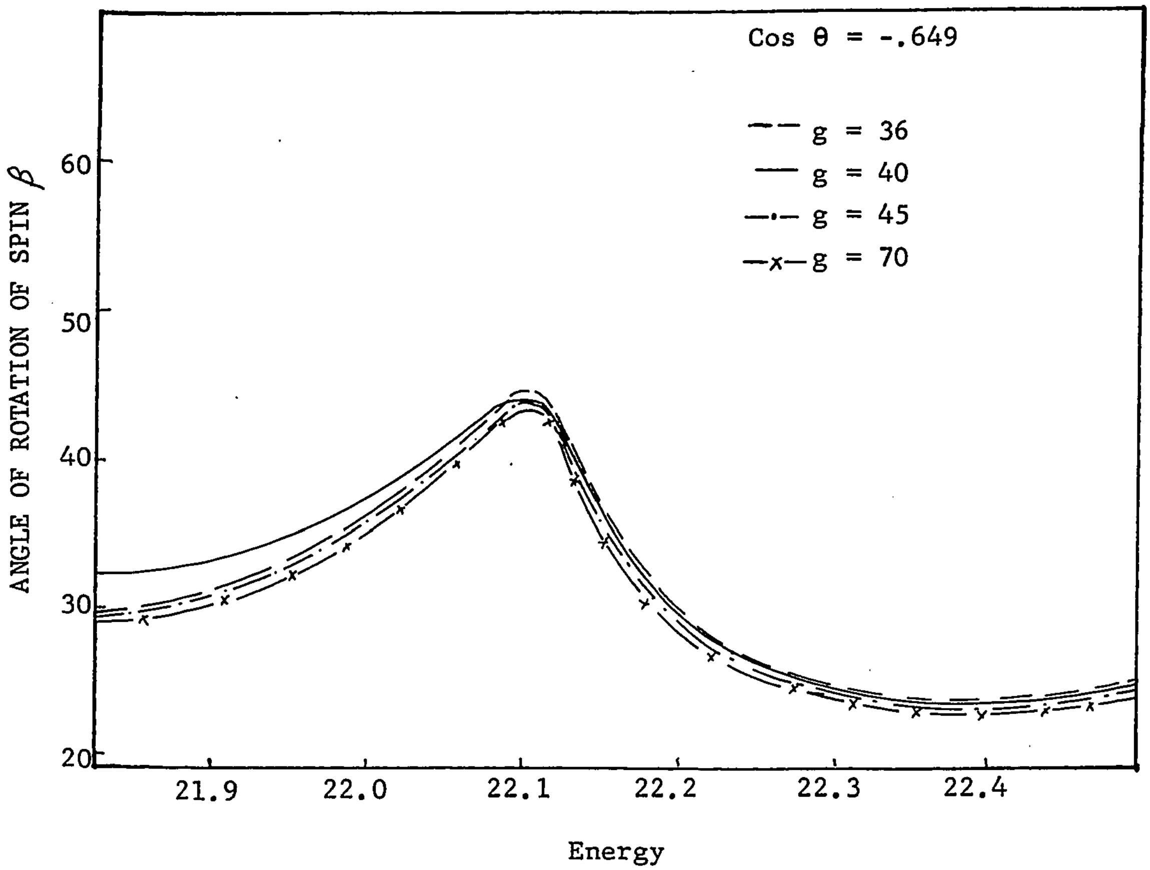

Figure XXIII. Angle of Rotation of Spin vs the Incident Neutron Energy. The angle is in the center-of-mass system. The incident neutron energy is in the laboratory system.

Reproduced with permission of the copyright owner. Further reproduction prohibited without permission.

Figures XXIV and XXV. Polarization vs Incident Neutron Energy. The incident neutron energy is in the laboratory system.

Reproduced with permission of the copyright owner. Further reproduction prohibited without permission.

POLARIZATION VS ENERGY

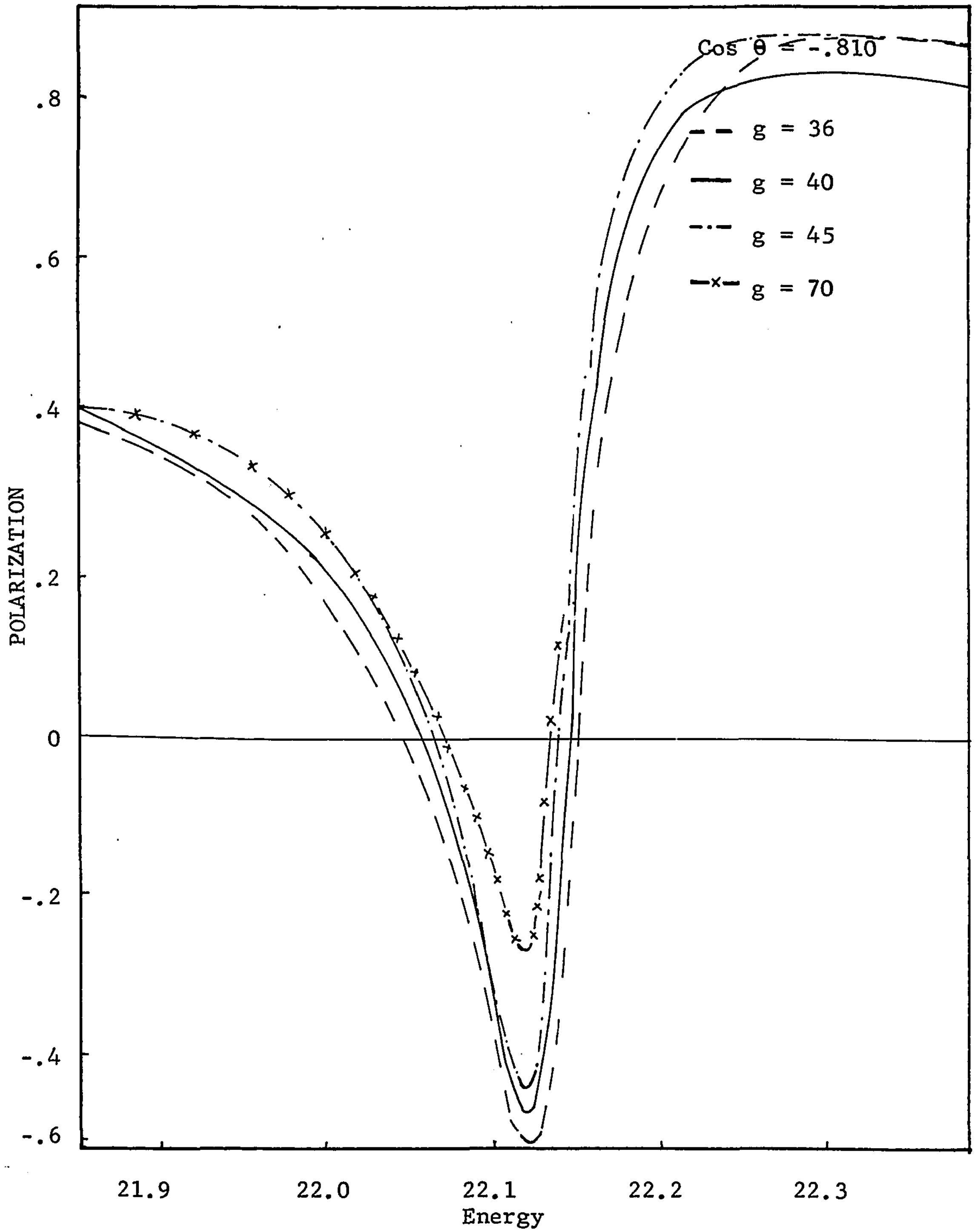

Figure XXIV

Reproduced with permission of the copyright owner. Further reproduction prohibited without permission.

POLARIZATION VS ENERGY

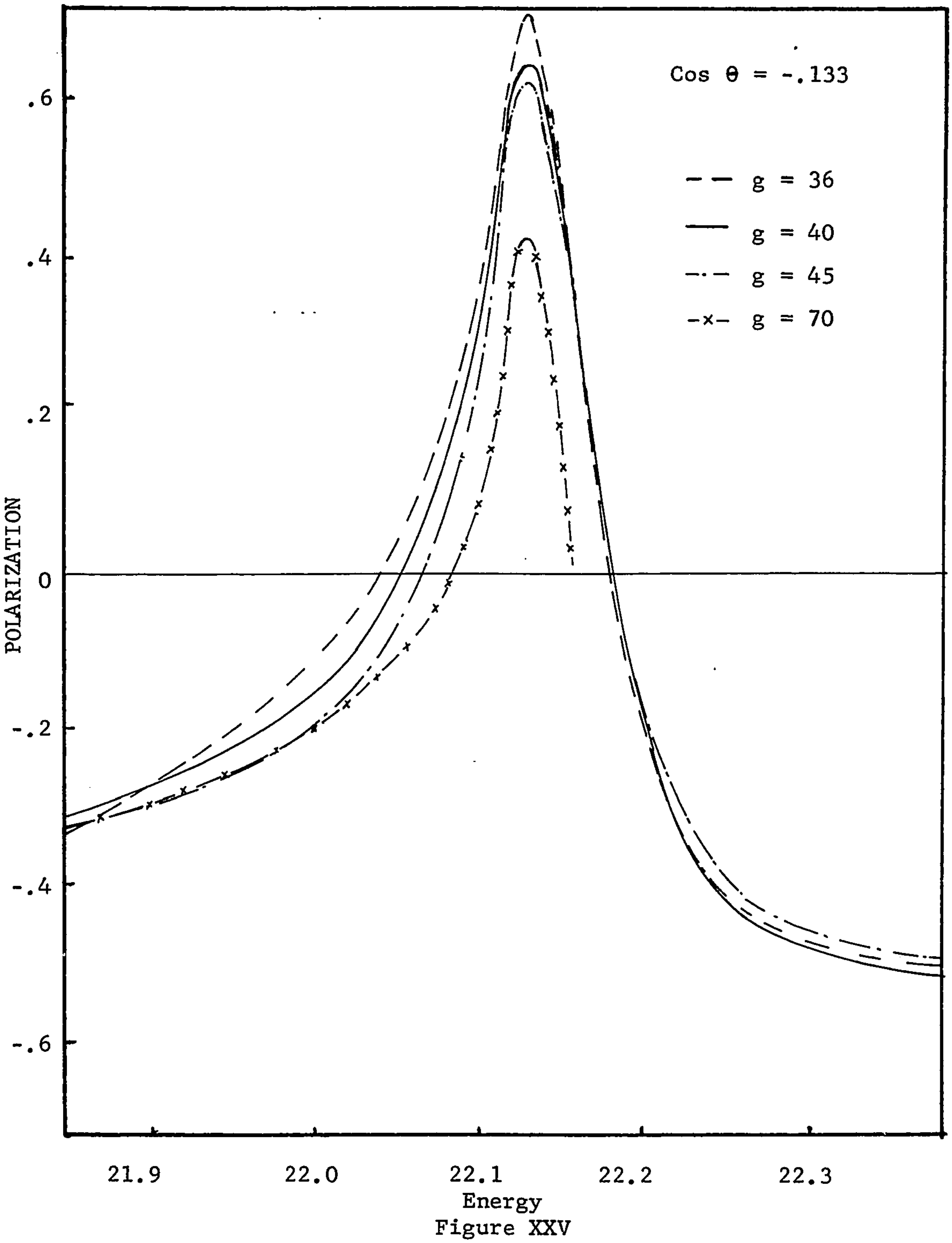

Figure XXV

Reproduced with permission of the copyright owner. Further reproduction prohibited without permission.

SUMMARY AND CONCLUSIONS

The results presented in the previous two chapters may be summarized as follows. The neutron alpha data for the total scattering cross section (Fig. VIII and IX), total elastic scattering cross section (Fig. X and XI) and differential elastic scattering cross section at 22.15 MeV neutron energy (Fig. XX) appear to exclude the value $\gamma_d^2/\gamma_n^2 = 70$ for the 16.7 MeV level of ^{5}He. The differential elastic scattering cross section data as a function of energy and as a function of angle (Fig. XII--XX) appear to exclude a value of g = 36. The total scattering cross section and the total elastic scattering cross section data are in good agreement with the calculations for both g = 40 and g = 45. However, the differential cross section data favor the value of $\gamma_d^2/\gamma_n^2 = 45$.

One might ask what further measurements might substantiate the value of g = 45 for the 16.7 MeV level in ^{5}He. The results of chapters 4 and 5 have bearing on what further measurements one might choose. These results indicate that measurements of the polarization and the angle of rotation of spin for neutron-alpha scattering are no more sensitive to the value of g than the total cross section, the total elastic cross section or the differential elastic scattering cross section.

A value of g = 45 supports the assumption that $\Gamma_n/\Gamma_d < 1$ at the resonance for the 16.7 MeV level in ^{5}He. This is in agreement with the results of Hoop and Barschall[10].

Reproduced with permission of the copyright owner. Further reproduction prohibited without permission.

A value of g = 45 for the 16.7 MeV level of ^5He is also consistent with the work of Balasko and Barit[14] and with one of the values suggested by Weitkamp and Haeberli[11] for the analogue level in ^5Li. Thus, if the value of g is indeed equal to 45 for the analogue state in ^5Li, then the results of the present work support the strong statement of charge symmetry.

However, present analyses are unable to confirm the value of g = 45 for the ^5Li system (See Table I). As pointed out by Weitkamp and Haeberli[11], only one of three groups of d (He^3, p) He^4 reaction cross section data favors the value $\gamma_d^2 / \gamma_n^2 = 45$. The other two groups of data favor g = 53[11] and g = 70[11]. Also, it does not appear possible to decide which value of g is correct, and thus which set of reaction data is correct on the basis of existing measurements of the polarization[16,26] and the differential elastic cross section data[15,25] for proton-alpha scattering. Clearly the parameters for ^5Li must be fixed before any firm conclusion may be drawn about the correctness of the strong statement of charge symmetry for the ^5He-^5Li system. Thus a precise measurement of the He^3 (d,p) He^4 reaction cross section is badly needed.

Reproduced with permission of the copyright owner. Further reproduction prohibited without permission.

APPENDIX A

Neutron-Alpha Phase Shifts and Inelastic Parameters

These phase shifts and inelastic parameters were published by Hoop and Barschall[10]. Common spectroscopic notation is used i.e. S, P, D, F refer to the orbital angular momentum, $\ell = 0, 1, 2, 3$ and 4 respectively, the subscript refers to total angular momentum $J = \ell \pm 1/2$. The $D_{3/2}$ phase shift is consistent with a value of the reduced width such that $\gamma_d^2 = 2$ MeV and g = 40. The symbol E_n designates the incident neutron energy. Only the $D_{3/2}$ inelastic parameters are listed because the inelastic parameters for the other levels are unity over this energy range.

Phase Shifts and Inelastic Parameter

E_n	$S_{1/2}$	$P_{1/2}$	$P_{3/2}$	$D_{3/2}$	$\tau_{3/2}$	$D_{5/2}$	$F_{5/2}$	$F_{7/2}$
21.6	89.0	53.0	92.0	10.0	1.00	10.0	3.0	3.0
21.85	89.0	53.0	92.0	11.75	1.00	10.0	3.0	3.0
21.90	89.0	53.0	92.0	15.0	1.00	10.0	3.0	3.0
22.0	89.0	53.0	92.0	19.0	1.00	10.0	3.0	3.0
22.05	89.0	53.0	92.0	24.0	1.00	10.0	3.0	3.0
22.09	89.0	53.0	92.0	32.0	.981	10.0	3.0	3.0
22.10	89.0	53.0	92.0	38.0	.919	10.0	3.0	3.0
22.11	89.0	53.0	92.0	44.0	.825	10.0	3.0	3.0
22.12	89.0	53.0	92.0	50.0	.70	10.0	3.0	3.0

Reproduced with permission of the copyright owner. Further reproduction prohibited without permission.

Phase Shifts and Inelastic Parameter Cont.

E_n	$S_{1/2}$	$P_{1/2}$	$P_{3/2}$	$D_{3/2}$	$\tau_{3/2}$	$D_{5/2}$	$F_{5/2}$	$F_{7/2}$
22.13	89.0	53.0	92.0	56.0	.492	10.0	3.0	3.0
22.14	89.0	53.0	92.0	58.0	.30	10.0	3.0	3.0
22.15	89.0	53.0	92.0	58.0	.154	10.0	3.0	3.0
22.16	89.0	53.0	92.0	37.0	.044	10.0	3.0	3.0
22.17	89.0	53.0	92.0	-6.0	.104	10.0	3.0	3.0
22.18	89.0	53.0	92.0	-10.0	.195	10.0	3.0	3.0
22.19	89.0	53.0	92.0	-10.0	.269	10.0	3.0	3.0
22.20	89.0	53.0	92.0	-9.0	.332	10.0	3.0	3.0
22.23	89.0	53.0	92.0	-6.0	.472	10.0	3.0	3.0
22.26	89.0	53.0	92.0	-5.0	.561	10.0	3.0	3.0
22.30	88.0	53.0	91.0	-2.0	.632	10.0	3.0	3.0
22.42	88.9	53.0	91.5	0.0	.71	10.0	3.0	3.0
22.60	88.0	53.0	91.0	2.0	.74	10.0	3.0	3.0

Reproduced with permission of the copyright owner. Further reproduction prohibited without permission.

APPENDIX B

The Principal of Reciprocity

The cross section of an inverse reaction is given by Evans[35] as:

$$\sigma(B \rightarrow A) = \frac{(2I_a + 1)(2I_b + 1)}{(2I_c + 1)(2I_d + 1)} \frac{P_a^2}{P_b^2} \sigma(A \rightarrow B)$$

where P_a is the momentum of the incident particle, P_c is the momentum of the lighter decay particle and I is the total angular momentum. Here, b designates the target particle; c, the heavier of the product particles. And, $\sigma(A \rightarrow B)$ is the cross section of the reaction going from A to B where A is the incident particle plus the target and B is the resulting nucleus plus the decay product.

Reproduced with permission of the copyright owner. Further reproduction prohibited without permission.

APPENDIX C

Computer Program for the Cross Sections

The following computer program is written in Fortran II for a 1620 IBM computer. It will calculate and punch out a total cross section, a total elastic cross section, a reaction cross section and the differential cross section at a given laboratory energy of the incident particle, provided it is given; the phase shifts and inelastic parameters up to $\lambda = 4$; the rest masses of the incident and target particle; the laboratory energy; and the angles at which the differential cross sections are to be calculated. The calculations will be relativistically correct to a first order approximation.

The following is a listing and definition of the terms in the program:

SMALM	Mass of the incident particle.
BIGM	Mass of the target particle.
N	Number angles at which the differential cross section is to be calculated.
TH(I)	Scattering angle θ at which the differential cross section will be calculated.
ENERG	Laboratory energy of the incident particle.
D(L)	Phase shift.
G(L)	Inelastic Parameter.
BLAM	Reciprocal of the wave number squared.
S(I)	Sine θ.
C(I)	Cos θ.

Reproduced with permission of the copyright owner. Further reproduction prohibited without permission.

P(I,L)	Legendre Polynomial.
PP(I,L)	Derivative of the Legendre Polnomial with respect to cos θ.
DRAD(L)	Phase shift in radians.
SDPA(L)	Sine of the phase shift.
CDPA(L)	Cosine of the phase shift.
REG(I)	Real part of the coherent amplitudes.
UNG(I)	Imaginary part of the coherent amplitudes.
REH(I)	Real part of the incoherent amplitudes.
UNH(I)	Imaginary part of the incoherent amplitudes.
DSDO(I)	Differential Cross Section.
POL(I)	Polarization.
BETA	Rotation Parameter.
CROSE	Total Elastic Scattering Cross Section.
CROSI	Inelastic Scattering Cross Section.
CROST	Total Cross Section.

Below is a listing of the program followed by a sample set of data. The data must be arranged as shown in the sample.

The .1 card indicates to the machine that this is the end of the job. If one would want to read in a completely different set of parameters, different masses or different angles, then the .1 card should be replaced by a .5 card followed by the new parameters as illustrated below.

Reproduced with permission of the copyright owner. Further reproduction prohibited without permission.

```
C     N-ALPHA DATA ANALYSIS    PHYSICS DEPT         DAVID GEORGE
      DIMENSION TH(40), D(7),G(7),S(40),C(40)
      DIMENSION UNG(40), REH(40), UNH(40), DSDO(40), POL(40), BETA(40)
      DIMENSION P(40,7), PP(40,7), DRAD(7), SDPA(7), CDPA(7), REG(40)
      DIMENSION RP(40)
      DIMENSION BR(7), DU(7), CO(7)
10    READ 1, SMALM, BIGM, N
1     FORMAT(F10.6,F10.6,I2)
      READ 21,(TH(I),I=1,N)
21    FORMAT(7F10.3)
41    READ 40,ENERG
40    FORMAT (F10.3)
      IF (ENERG-1.0) 42,43,43
43    CONTINUE
      READ 3,(D(L),G(L),L=1,7)
3     FORMAT(8F10.3)
C     CALCULATE 1/K**2
      WA=0.0
      WA=.000537*(1.-SMALM/BIGM)**2
      BLAM=0.0
      BLAM=(209.07/SMALM)*(((1.+SMALM/BIGM)**2)/ENERG-WA)
C     CALCULATE LEGENDRE POLYNOMIALS
      PI= 3.1415926
      DO 45 I=1,N
      TH(I) = TH(I)* PI/180.0
      S(I)= SINF (TH(I))
      C(I)= COSF(TH(I))
      P(I,1)= 0.5
      P(I,2)=0.5*C(I)
      P(I,3)= C(I)
      P(I,4)=1.5* C(I)**2-0.5
      P(I,5)=1.5*P(I,4)
      P(I,6)= 3.75*C(I)**3-2.25*C(I)
```

Reproduced with permission of the copyright owner. Further reproduction prohibited without permission.

```
      P(I,7)= P(I,6)*4.0/3.0
C     CALCULATE DERIVATIVES OF LEGENDRE POLYNOMIALS
      PP(I,1)=0.0
      PP(I,2)=0.5*S(I)
      PP(I,3)=-PP(I,2)
      PP(I,4)= 1.5* S(I)*C(I)
      PP(I,5)=-PP(I,4)
      PP(I,6)= S(I)*(3.75*C(I)**2-0.75)
      PP(I,7)=-PP(I,6)
   45 TH(I)= TH(I)*180.0/PI
C     CALCULATE DIFFERENTIAL CROSSECTION
      DO 50 L=1,7
      DRAD(L)=D(L)*PI/90.00
      SDPA(L) = SINF(DRAD(L))
      CDPA(L) = COSF(DRAD(L))
      BR(L) = G(L)* SDPA(L)
      BU (L) = G(L)* CDPA(L) - 1.0
   50 CONTINUE
      DO 65 I=1,N
      REG(I)=0.0
      UNG(I) =0.0
      REH(I) =0.0
      UNH (I) =0.0
      DO 60 L=1,7
      REG(I)= REG(I) + P(I,L)* BR(L)
      UNG (I)= UNG(I) - P(I,L)* BU(L)
      REH(I) = REH(I)+ PP(I,L) * BR(L)
   60 UNH(I) = UNH(I) - PP(I,L)* BU(L)
      DSDO(I) = BLAM*(REG(I)**2+UNG(I)**2+REH(I)**2+UNH(I)**2)
      POL(I)=2.0*(REG(I)*UNH(I)-UNG(I)*REH(I))*BLAM/     DSDO(I)
      BETA(I)=ATANF(2.0*(REH(I)*REG(I)+UNG(I)*UNH(I))*BLAM/DSDO(I))
      RP(I)= BETA(I)*180.0/PI
```

Reproduced with permission of the copyright owner. Further reproduction prohibited without permission.

```
65    CONTINUE
C     CALCULATE ELASTIC CROSSECTION
C     DIFINE COEFFICIENTS
      CO(1)=1.0
      CO(2)=1.0
      CO(3)= 2.0
      CO(4)=2.0
      CO(5)= 3.0
      CO(6)=3.0
      CO(7)=4.0
      CROSE=0.0
      CROSI=0.0
      CROST=0.0
      DO 80 L=1,7
      CROSE= CROSE + CO(L)*(-1.0+G(L)**2-2.0*BU(L))*PI*BLAM
      CROSI = CROSI + CO(L) *(1.0 - G(L)**2)*PI*BLAM
80    CONTINUE
85    FORMAT(8HENERG = ,F10.3,4H MEV)
      CROST=CROSE+CROSI
      PUNCH 85, ENERG
      PUNCH 87
87    FORMAT(15X,4HS1/2,6X,4HP1/2,6X4HP3/2,6X,4HD3/2,6X,4HD5/2,6X,
     G 4HF5/2,6X,4HF7/2)
      PUNCH 88,(D(L),L=1,7)
88    FORMAT(8HPHAS SFT,7F10.3)
      PUNCH 89,(G(L),L=1,7)
89    FORMAT(6HINEL PAR,7F10.3)
      PUNCH 86,CROST,CROSE,CROSI
86    FORMAT(11HTOT XSECT =,F10.3,12HELAS XSECT =,F10.3,
     G   14HINELAS XSECT =,F10.3)
      PUNCH 91
91    FORMAT(9HCOS THETA, 5X,13HDIFF CROSSECT, 3X,6H   POL,
```

Reproduced with permission of the copyright owner. Further reproduction prohibited without permission.

```
      G  7X, 8H ROT PAR)
       DO 92 I=1,N
       PUNCH 93, C(I), DSDO(I), POL(I), RP(I)
93     FORMAT(F10.3,5X,F10.3,5X,F10.3,5X,F10.3)
92     CONTINUE
       GO TO 41
42     CONTINUE
       IF(ENERG - .1) 100,101,100
100    GO TO 10
101    CONTINUE
       PUNCH 525, SMALM, BIGM, N
525    FORMAT(F10.6,F10.6,I2)
       CALL EXIT
       END
  1.008962   4.00260008
    69.5      82.7      97.7      108.9      119.7  130.5      144.16
    152.05
    22.10
    89.0      1.0       53.0      1.0        92.0      1.0      37.4      .98
    10.0      1.0       3.0       1.0        3.0      1.0
    0.5
  1.008982  4.00260  37
    0.0       5.0       10.0      15.0       20.0      25.0      30.0
    35.0      40.0      45.0      50.0       55.0      60.0      65.0
    70.0      75.0      80.0      85.0       90.0.     95.0      100.0
    105.0     110.0     115.0     120.0      125.0     130.0     135.0
    140.0     145.0     150.0     155.0      160.0     165.0     170.0
    175.0     180.
    22.0
    89.0      1.0       53.0      1.0        92.0      1.0       18.91     1.0
    10.0      1.0       3.0       1.0        3.0       1.0
    .10
```


Reproduced with permission of the copyright owner. Further reproduction prohibited without permission.

BIBLIOGRAPHY

1. L. Heller, Phys. Rev. 39, 584 (1967).

2. L. Heller, P. Signell and N. R. Yoder, Phys. Rev. Letters 13, 577 (1964).

3. Haddock, R. M. Salter Jr., M. Zeller, J. B. Czirr and D. R. Nygren, Phys. Rev. Letter 3, 304 (1963).

4. L. R. B. Elton, Introductory Nuclear Theory, W. B. Saunders Company, Philadelphia, 1966, pp. 30 and 85.

5. G. Breit, "Theory of Resonance Reactions and Allied Topics," Handbuck der Physik, S. Flügge, ed., Berlin, 1959, Vol. XLI/1 p. 237.

6. J. P. Conner, T. W. Bonner and J. R. Smith, Phys. Rev. 88, 468 (1952).

7. W. E. Kunz, Phys. Rev. 97, 456 (1955).

8. T. Lauritsen and F. Ajzenberg-Selove, Nucl. Phys. 78, 1 (1966).

9. I. G. Balashko and I. I. Barit, Nuclear Forces and the Few-Nucleon Problem, T. G. Griffith and E. A. Power, ed., Pergamon Press, New York, 1960, Vol. 2, p. 615.

10. B. Hoop Jr., and H. H. Barschall, Nucl. Phys. 83, 65 (1966).

11. W. G. Weitkamp and W. Haeberli, Nucl. Phys. 83, 46 (1966).

12. H. V. Argo, R. F. Taschek, H. M. Agnew, A. Hemmendinger and W. T. Leland, Phys. Rev. 87, 612 (1952).

13. J. L. Yarnell, R. H. Lovberg and W. R. Stratton, Phys. Rev. 90, 292 (1953).

14. A. P. Klincharev, B. N. Esel'son and A. K. Val'ter, Doklady (Soviet Physics) 1, 475 (1956).

15. P. W. Allison and R. Smythe, Bull. Am. Phys. Soc. 9, 544 (1964).

16. M. K. Craddock, R. C. Hanna, L. P. Robertson and B. W. Davis, Phys. Letters 5, 335 (1963).

17. T. W. Bonner J. P. Conner and A. B. Lillie, Phys. Rev. 88, 473 (1952).

Reproduced with permission of the copyright owner. Further reproduction prohibited without permission.

18. G. Frier and H. Holmgren, Phys. Rev. 93, 825 (1954).

19. D. L. Both, R. S. Hill, F. V. Price and D. Roaf, Phys. Soc. (London) A 70, 863 (1957).

20. R. E. Shamu and J. G. Jenkin, Phys. Rev. 135, B99 (1964).

21. R. E. Benenson, D. B. Lightbody, A. Sayres and W. E. Stephens, Bull. Am. Phys. Soc. (London) 10, 52 (1962).

22. H. H. Barschall, Nucl. Phys. 83, 65 (1966).

23. L. Wolfenstein, Am. J. Phys. 35, 119 (1966).

24. M. J. Moravicsik, The Two-Nucleon Interaction, Clarendon Press, Oxford, 1963, p. 20.

25. P. W. Allison, Ph. D. Thesis, University of Colorado.

26. National Institute for Research in Nuclear Science (U.K.) P.L.A. Progress Report (1963).

27. I. G. Balashio and I. I. Barit, Soviet Physics: JETP, 7, 715 (1958).

28. E. Merzbacher, Quantum Mechanics, J. Wiley and Sons, Inc., New York, 1961, p. 215.

29. P. G. Burke, Nuclear Forces and the Few-Nucleon Problem, T. G. Griffith and E. A. Power, ed., Pergamon Press, New York, 1960.

30. J. M. Blatt and V. F. Weisskopf, Theoretical Nuclear Physics, J. Wiley and Sons, New York, 1952.

31. W. S. Porter, B. Roth and J. L. Johnson, Phys. Rev. 3, 1578 (1958).

32. A. M. Lane and R. G. Thomas, Rev. Mod. Phys. 30, 257 (1958).

33. J. H. Coon and R. W. Davis, Bull. Am. Phys. Soc. 4, 366 (1959).

34. H. B. Willard, L. C. Biedenharn, P. Huber and E. Baumgartner, Fast Neutron Physics, J. B. Marion and J. L. Fowler, ed., Interscience Publishers, Inc., New York, 1963, Part II, p. 1222.

35. R. D. Evans, The Atomic Nucleus, McGraw-Hill, New York, 1955, p.333.

36. P. Morrison, Experimental Nuclear Physics, E. Segre, ed., John Wiley and Sons, New York, 1953, Vol. 2, p. 10.

Reproduced with permission of the copyright owner. Further reproduction prohibited without permission.

37. T. Lauritsen and F. Ajzenberg-Selove, Nucl. Phys. 78, 1 (1966).

38. I. Bloch, M. M. Hull, A. A. Broyles, W. G. Bouricius, B. E. Freeman and G. Breit, Rev. Mod. Phys. 23, 147 (1951).

39. W. T. Sharp, H. E. Gove and E. B. Paul, Graphs of Coulomb Functions, TPI-70, Atomic Energy of Canada Limited, Chalk River, Ontario, AECL-268 (1961).

40. G. Westin, M. A. Thesis, Western Michigan University, 1965.

41. M. E. Rose, Phys. Rev. 91, 610 (1953).

42. L. G. Lawrence, Australian National University Report, ANU-P/287, (unpublished).

43. P. B. Perkins, (private communication) to J. G. Jenkin.

44. J. G. Jenkin and R. E. Shamu, Nucl. Inst. and Meth. 34, 116-120 (1965).

Reproduced with permission of the copyright owner. Further reproduction prohibited without permission.